



# SHIODEG: a hybrid success-history intelligent optimization algorithm for engineering design problems

Sadi Alawadi<sup>1</sup> · Hussam N. Fakhouri<sup>2</sup> · Fahed Alkhabbas<sup>3</sup> · Victor R. Kebande<sup>1</sup> · Feras M. Awaysheh<sup>4</sup> · Abbas Cheddad<sup>4</sup>

Received: 26 July 2025 / Accepted: 20 February 2026  
© The Author(s) 2026

## Abstract

This paper proposes SHIODEG, a hybrid metaheuristic that integrates the success-history intelligent optimizer (SHIO) with differential evolution (DE) and a Gaussian transformation (GT) to tackle two persistent challenges in optimization for engineering design: (i) the absence of a universally best optimizer across problem classes (as implied by the No-Free-Lunch perspective) and (ii) the limited ability of purely gradient-based methods to produce substantial improvements in complex, constrained, and often non-smooth real-world problems, motivating hybrid strategies that balance exploration and exploitation. SHIODEG follows a staged search process in which DE generates diverse trial solutions, GT injects normally distributed perturbations to reduce premature convergence and diversity collapse, and SHIO refines promising regions using success-history guidance from the best three leaders. SHIODEG is evaluated on the IEEE CEC2022 benchmark suite (12 functions) using 30 independent runs, a population size of 100, and a budget of 1000D function evaluations. The results show that SHIODEG consistently delivers top-tier performance across the benchmark suite, showing strong competitiveness, low variability, and statistically significant improvements over a wide range of alternative optimizers. It also demonstrates robust effectiveness on multiple constrained engineering design problems, achieving high-quality solutions across diverse real-world constraints.

**Keywords** Success-history intelligent optimizer · Gaussian transformation · Differential evolution · Optimization

## 1 Introduction

Swarm intelligence (SI) has emerged as a critical sub-field of artificial intelligence (AI), drawing inspiration from the collective behavior of decentralized, self-organized systems, particularly those observed in human and animal social dynamics [1]. SI encompasses a broad set of algorithms that are characterized by the coordination

---

Extended author information available on the last page of the article

of individual agents in a population to collectively solve complex problems [2]. These problems often mirror natural phenomena, such as the flocking of birds, the foraging behavior of ants, or the schooling of fish, and span various domains from robotic control to task scheduling and optimization [3]. Central to SI is its profound role in addressing complex optimization problems. In an era where systems are growing increasingly intricate and high-dimensional, optimization tasks are becoming more challenging to solve [4]. With their inherent decentralized structure and flexibility, SI-based algorithms have demonstrated an impressive capability to tackle such issues, bridging the gap between theoretical complexity and real-world practicality [5]. In fact, SI-based algorithms offer several advantages over traditional methods, such as robustness to changing environments, adaptability, scalability, and resilience to failure, making them an ideal choice for solving a myriad of optimization problems [6]. However, as the field of AI continues to evolve, so does the demand for more efficient, powerful, and adaptable SI algorithms. Existing intelligent algorithms, while effective, still suffer from certain limitations such as slow convergence rate, stagnation in local optima, and lack of diversity in search space exploration [7].

Recent research in metaheuristic optimization has increasingly shifted from proposing entirely new metaphors to systematically *enhancing* existing optimizers through well-established improvement strategies. Three particularly active directions include: (i) *adaptive mechanisms* (e.g., success-history or feedback-driven parameter/position control), (ii) *multi-strategy integration* (e.g., hybridizing complementary search operators within a single framework), and (iii) *distribution-based perturbation* (e.g., injecting stochastic steps via Gaussian or heavy-tailed random walks to preserve diversity and escape local optima). Representative recent examples include an adaptive position-updating PSO for UAV path planning [8], an enhanced red-billed blue magpie optimizer [9], and an enhanced whale optimizer combining Levy and spiral flights [10]. Motivated by these trends, SHIODEG is designed as a unified enhancement framework: SHIO contributes success-history learning (adaptive guidance), DE contributes robust variation/selection operators (multi-strategy integration), and GT contributes normally distributed perturbations (distribution-based exploration).

The key challenges addressed in this paper are summarized as follows: First, there is a lack of a one-size-fits-all solution in optimization algorithms, as has been highlighted by the No-Free-Lunch theorem that not only underscores the fundamental reality in optimization algorithms but also shows the relevance of developing specialized algorithms that are fine-tuned to a particular class of problems [11, 12]. Second, traditional gradient-based optimization techniques are not sufficient to substantially optimize real-world engineering issues. Therefore, there is a need to develop a hybrid optimizer that combines the features of more than one optimizer to solve such problems.

To address these challenges, we propose the success-history intelligent optimizer (SHIO), with Gaussian transformation (GT) and differential evolution (DE), hereafter referred to as SHIODEG, a hybrid algorithm that combines the strengths of DE and Gaussian transformation. This integration fosters more efficient and effective optimization solutions, which enhance SHIO exploration of the further capabilities

that can be exploited, especially when dealing with complex engineering design problems.

- **A unified hybrid framework:** We introduce SHIODEG, which integrates SHIO, DE, and GT in a staged search strategy to balance exploration and exploitation.
- **Diversity-preserving perturbation:** We incorporate Gaussian perturbations to reduce premature convergence and maintain population diversity during the search.
- **Comprehensive validation:** We evaluate SHIODEG on the IEEE CEC2022 benchmark suite and on constrained engineering design problems, supported by statistical testing against state-of-the-art optimizers.

The remainder of this paper is organized as follows: Section 2 reviews related work in metaheuristic optimization in detail. Section 3 introduces the proposed SHIO-DEG algorithm, including its formulation and main components. Section 4 presents the experimental setup and discusses the results on benchmark functions and real-world engineering design problems. Section 5 discusses the proposed algorithm and its limitations. Finally, Sect. 6 concludes the paper and outlines future research directions.

## 2 Related work

Metaheuristic optimization has been widely developed by borrowing mechanisms from diverse sources such as human activities, natural and biological processes, physical phenomena, strategic principles, and abstract mathematical concepts [13]. These inspiration routes have produced a large ecosystem of population-based optimizers as well as a parallel literature on enhancement strategies that target common weaknesses such as premature convergence, loss of diversity, and slow refinement.

A substantial family of methods explicitly models social or human-centered processes. Cultural algorithms (CA) formalize the way societies accumulate and transmit shared knowledge during problem-solving [14]. Human behavior-based optimization (HBBO) similarly abstracts collective human behaviors into search operators that represent exploration and exploitation in decision-making contexts [15]. Other examples use more specific social metaphors: political optimizer (PO) mimics campaign strategies and competing parties to drive competitive search [16], while teaching-learning-based optimization (TLBO) translates classroom learning dynamics into iterative improvement rules [17]. At a finer granularity, Chef-Based Optimization Algorithm (CBOA) models chefs' decision processes (e.g., choosing ingredients/recipes) as a structured search procedure [18], whereas Fans optimization (FO) and mother optimization algorithm (MOA) capture supportive and nurturing behaviors to guide candidate solutions toward better regions [19, 20]. Collectively, these studies illustrate a recurring pattern: designing stage-based dynamics that progressively shift from broad exploration to focused exploitation through role-based interactions.

Beyond human metaphors, several optimizers rely on abstract operators and system dynamics. Arithmetic optimization algorithm (AOA) uses arithmetic operators as primary search primitives to modulate exploration and exploitation [21], while Chaos Game Optimization (CGO) leverages chaotic behavior to generate diverse trajectories across the search space [22]. Supply–demand-based optimization (SDO) adopts economic supply–demand interactions to adaptively adjust search pressure [23]. In parallel, well-established animal-inspired methods remain influential baselines and building blocks: Artificial Bee Colony (ABC) mimics foraging behaviors [24], Ant Colony Optimization (ACO) exploits pheromone-mediated path construction [25], Particle Swarm Optimization (PSO) models social movement in flocks and schools [26], and Grey Wolf Optimizer (GWO) captures hierarchical hunting roles and encircling strategies [27]. These canonical frameworks often motivate later enhancements through improved initialization, adaptive control, and perturbation mechanisms.

A focused stream of related work concerns enhanced variants of Whale optimization algorithm that aims to strengthen convergence and robustness. RWOA introduces Good Nodes Set initialization and hybrid collaborative exploration combined with Lévy-flight-based spiral updating to improve accuracy and convergence speed on benchmark functions and engineering designs [28]. GWOA integrates adaptive parameter tuning, an improved prey-encircling mechanism, and sine–cosine search patterns to enhance global search capability and convergence efficiency in complex engineering tasks [29]. More recently, LSEWOA combines enhanced initialization, dynamic guided search, and improved spiral updates, reporting strong performance across diverse numerical benchmarks and engineering design challenges [30]. Taken together, these WOA studies exemplify a broader trend: baseline metaheuristics are increasingly upgraded using multi-strategy combinations (e.g., better initialization, guided exploitation, and heavy-tailed perturbations) to reduce stagnation and sensitivity to problem structure.

Recent contributions can be usefully grouped along three complementary dimensions: (i) the *inspiration and induced search dynamics* (bio/nature-, physics/space-, human-process-, and math/gradient-inspired), (ii) the *algorithmic form* (stand-alone, enhanced, hybrid, or deterministic), and (iii) the *deployment context* (benchmark-centered validation versus domain-embedded optimization in engineering and machine learning pipelines). This viewpoint helps connect metaphor-driven proposals with practical design choices such as parameter adaptation, constraint handling, and representation-aware operators.

Bio- and nature-inspired stand-alone methods continue to propose novel movement and selection rules to better balance exploration and exploitation. KOA models kakapo roaming and zigzag navigation for exploration and integrates exploitation behaviors such as freezing/camouflage with elitist survival selection, reporting competitive performance on CEC2017 [31]. BBLA encodes defensive/foraging behaviors of black-breasted lapwings into lightweight operators and shows strong benchmark performance as well as effectiveness on constrained engineering designs (e.g., spring, welded beam, and pressure vessel problems) [32]. CLO introduces multi-stage search and dynamic information exchange inspired by cape lynx behaviors, demonstrating competitive CEC2017 results and strong wireless sensor network

coverage performance under different environmental scenarios [33]. Natural-phenomenon metaphors also remain active: the Raindrop Optimizer (RD) decomposes search into distinct exploration processes (e.g., splash and diversion) and exploitation processes (e.g., convergence and overflow) and demonstrates usefulness both on benchmarks and in robotic filter/controller tuning [34].

Physics- and space-inspired designs increasingly seek principled updates and broader evaluations. The Centered Collision Optimizer (CCO) derives update rules from collision mechanics and couples operations in the original and decorrelated spaces with allocation strategies to speed convergence; it is evaluated across multiple CEC suites, constrained engineering designs, photovoltaic parameter identification, and real-world constrained sets [35]. The Aurora optimizer uses charged particle dynamics and magnetic-field-inspired mechanisms (aurora phenomena) with best-solution guidance to balance exploration and exploitation, reporting strong benchmark and engineering design performance [36]. In addition, a notable push toward reproducibility is reflected in the three-body deterministic optimizer (TBD), which removes stochastic operators and instead relies on orbital-mechanics-inspired maneuvers with logistic-map-driven (yet reproducible) dynamics; TBD is evaluated on CEC2017/2022 and applied to CNN hyperparameter tuning [37]. Human-process and math/gradient-inspired variants further broaden this landscape: TJO structures the search as phases of jam formation, driver self-regulation, and enforcement, illustrating how staged transitions can gradually intensify exploitation [38]. AGDO borrows the momentum-like memory and adaptive update spirit of Adam while maintaining a population-based metaheuristic form, reporting strong results on CEC2017 and applications spanning continuous engineering and discrete scheduling contexts [39].

Hybridization is repeatedly used to mitigate premature convergence and strengthen local refinement, particularly under constraints or discrete structure. HBFA combines exploration tendencies from Sunflower Optimization with exploitation mechanisms from Butterfly Optimization, reporting strong performance on standard benchmarks and constrained mechanical designs [40]. In parameter identification, hybridization can be applied more selectively: for LED lamp parameter estimation, ROA is first established as a strong baseline and then two hybrid ROA variants are introduced to improve speed and estimation quality, supported by robustness and harmonic analyses [41]. For discrete combinatorial settings, DFP-GA integrates flower pollination dynamics with genetic operators and adaptive conversion probability to reduce stagnation and improve sequence quality in assembly planning [42]. EPDO extends Prairie Dog Optimization with Lévy flights and adaptive phases to improve convergence and constraint satisfaction in QoS-aware cloud service composition [43]. Hybridization also increasingly appears as *meta-optimization* via guidance layers: an AI-guided framework for economic dispatch evaluates multiple underlying metaheuristics and reports improved reliability and convergence behavior on IEEE 30-bus dispatch problems [44]. These works collectively indicate that hybrid designs are often motivated by concrete failure modes (stagnation, weak exploitation, constraint handling) and are validated in both benchmarks and engineering deployments.

A major applied trend is to embed metaheuristics in end-to-end learning systems, where the optimizer tunes model hyperparameters, selects features, or solves domain decision problems via surrogate predictions. In sustainable materials design, an ensemble predictor models geopolymer compressive strength and a metaheuristic optimizer searches mixture proportions under multi-objective criteria (strength, cost, CO<sub>2</sub>, and energy) [45]. In dam-failure peak outflow prediction, random forests are tuned using multiple metaheuristics (including SSA, HHO, and GWO) to improve predictive accuracy and are paired with interpretability tools to identify the most influential physical drivers [46]. For renewable forecasting, a wind power pipeline couples dimensionality reduction (t-SNE), an enhanced gate-based LSTM, and a metaheuristic with intelligent position navigation to improve accuracy under seasonal variability [47]. Metaheuristic-driven feature selection can also serve as a pre-processing stage: a modified chaotic enriched Jaya–Moth Flame hybrid (MCEJ) performs extreme feature selection before LSTM-based software effort estimation [48]. Similarly, hybrid “metaheuristic + ANN” templates are used for energy conversion modeling, where ANN variants (e.g., ANN-THRO, ANN-BSLO, ANN-QIO) predict syngas species concentrations across gasification conditions [49]. More recently, metaheuristics have been paired with generative modeling: DentoSMART-LDM combines a tailored multi-objective metaheuristic (DSMART) for dental radiograph enhancement with a pathology-aware latent diffusion model (DentoLDM), targeting both enhancement quality and data scarcity while improving downstream diagnostic performance [50]. Overall, these studies highlight metaheuristics as flexible components for coordinating trade-offs that are difficult to express as single analytic objectives, especially in multi-objective and data-driven settings.

Across the literature, modern improvements can be summarized into three recurring mechanisms: *adaptive control*, *multi-strategy integration*, and *distribution-based perturbation*. Adaptive control uses feedback or memory to reduce sensitivity to fixed parameters; for example, a PSO variant employs dynamic inertia adjustment along with chaotic initialization and Lévy perturbations to improve convergence and local-optima avoidance in UAV path planning [51]. A related direction is adaptive position updating in PSO to improve efficiency and solution quality in application-driven UAV scenarios [8]. Multi-strategy integration combines complementary operators to balance exploration–exploitation and mitigate stagnation, exemplified by MRBMO as an enhanced red-billed blue magpie optimizer augmented with additional improvement mechanisms [9]. Distribution-based perturbations (e.g., Gaussian noise or heavy-tailed Lévy steps) remain widely used to preserve diversity and enable escapes from local optima; LSWOA demonstrates this idea by incorporating Lévy and spiral flight behaviors into WOA to improve global exploration while retaining exploitation capability [10]. These enhancement patterns align closely with recent WOA improvements that mix strong initialization, adaptive guidance, and perturbation operators [28–30].

Benchmark-centered validation (often using CEC suites) and constrained engineering design problems remain dominant evaluation settings for both stand-alone and hybrid proposals [35, 38–40]. Hybridization is repeatedly adopted to counter premature convergence, accelerate convergence, and adapt search to discrete or constrained structures [40–43]. In parallel, there is strong momentum toward embedding metaheuristics within learning pipelines for surrogate-assisted decision optimization, hyperparameter tuning, feature selection, and generative enhancement

[45–48, 50]. Finally, concerns about traceability and repeatability motivate deterministic alternatives such as TBD [37] and guidance-layer approaches that aim to improve reliability across different base optimizers [44]. In this context, SHIODEG is best interpreted as an enhancement-oriented framework that combines success-history learning (adaptive biasing), DE-style variation operators (robust diversity maintenance), and Gaussian perturbations (distribution-based exploration), consistent with the prevailing design directions in recent metaheuristic research [8–10, 51].

Metaheuristic optimization works can be organized along three complementary axes: (i) *inspiration and search dynamics* (bio/nature-, physics/space-, human-process-, and gradient-inspired), (ii) *algorithmic form* (stand-alone, hybrid/enhanced, and deterministic), and (iii) *deployment context* (benchmark-centric studies versus application-driven optimization embedded in machine learning and engineering pipelines). Table 1 summarizes a compact classification.

### 3 SHIODEG: our proposed hybrid algorithm

Hybrid metaheuristics aim to exploit complementary search behaviors by coupling operators with different strengths (e.g., exploration vs. exploitation), often improving robustness on complex and multimodal landscapes [52]. Following this principle, we propose *SHIODEG*, a tri-component hybrid that integrates: (i) differential evolution (DE) for population-difference exploration, (ii) Gaussian transformation (GT) as an explicit diversity injection mechanism, and (iii) success-history intelligent optimization (SHIO) as a leader-driven exploitation/refinement stage. The implementation of SHIODEG is publicly available on the MathWorks File Exchange.<sup>1</sup>

#### 3.1 Novelty and relation to prior hybrids

SHIODEG enforces a staged information flow

DE (global sampling) → GT (diversity injection) → SHIO (success-history exploitation),

which separates operator roles and reduces premature convergence risk. In contrast to existing two-component SHIO–GT variants (e.g., used in hyperparameter tuning [53]), SHIODEG introduces DE as a dedicated exploration engine and uses GT to prevent diversity collapse when DE steps become small during convergence. Compared with common DE/swarm hybrids that alternate operators without an explicit diversity “floor”, SHIODEG maintains non-vanishing stochastic exploration through Gaussian perturbations while reserving SHIO for exploitation around the best regions discovered by DE.

#### 3.2 Control parameters

SHIODEG is governed by the following parameters:

<sup>1</sup> <https://www.mathworks.com/matlabcentral/fileexchange/168366-shiodeg-a-hybrid-success-history-intelligent-optimization>.

**Table 1** Classification of the reviewed studies by inspiration, algorithmic form, and problem setting

Ref.	Optimizer framework	Inspiration	Form	Primary focus/setting
Khahre et al. [40]	HBFA	Nature (sunflower + butterfly)	Hybrid metaheuristic	Unimodal/multimodal benchmarks; constrained mechanical design
Wang and Shang [38]	Traffic Jam Optimizer (TJO)	Human/process (traffic control)	Stand-alone swarm	Global optimization (CEC2017); engineering problems
Lang et al. [35]	Centered Collision Optimizer (CCO)	Physics (collision mechanics)	Stand-alone physics-based	CEC2017/2019/2022; constrained engineering; PV parameter ID; real-world constrained set
Fakhouri et al. [36]	Aurora Optimizer	Space/physics (charged particles, magnetic fields)	Stand-alone swarm	Benchmarks (23/50 functions, CEC2022); engineering design
Chen et al. [34]	Raindrop Optimizer (RD)	Nature (raindrop phenomena)	Stand-alone nature-inspired	Benchmarks; robotic filter/controller tuning
Qawaqneh et al. [31]	Kakapo Optimization Algorithm (KOA)	Bio-inspired (kakapo behavior)	Stand-alone bio-inspired	CEC2017 suite; general optimization applications
Qawaqneh et al. [32]	Black-breasted Lapwing Algorithm (BBLA)	Bio-inspired (defense/foraging)	Stand-alone bio-inspired	Benchmarks; constrained engineering design
Wang and Yao [33]	Cape Lynx Optimizer (CLO)	Bio-inspired (lynx behaviors)	Stand-alone swarm	CEC2017; wireless sensor network coverage
Xia and Ji [39]	Adam Gradient Descent Optimizer (AGDO)	Math/gradient-inspired (Adam)	Stand-alone metaheuristic	CEC2017; continuous engineering; DFSP scheduling
Rodan et al. [37]	Three-body Deterministic Optimizer (TBD)	Physics + chaos (orbital mechanics)	Deterministic metaheuristic	CEC2017/2022; engineering design; CNN hyperparameter tuning
Micev et al. [41]	Hybrid ROA variants	Bio-inspired (Red Kite)	Hybrid metaheuristic	LED lamp parameter estimation (optimization-based ID)
Ding et al. [42]	DFFP-GA	Pollination + GA operators	Hybrid (discrete)	Assembly sequence planning (discrete optimization)
Tian [43]	EPDO	Bio-inspired + Lévy flights	Enhanced metaheuristic	QoS-aware cloud service composition under constraints

**Table 1** (continued)

Ref.	Optimizer framework	Inspiration	Form	Primary focus/setting
Su et al. [45]	Ensemble + DBO	Learning-assisted (ML + metaheuristic)	ML – metaheuristic pipeline	Multi-objective mix optimization (strength/cost/CO <sub>2</sub> /energy) for geopolymer

- **Population size** ( $N$ ): number of candidate solutions.
- **Maximum iterations** ( $L_{\max}$ ): termination budget (or equivalently, a function-evaluation budget).
- **DE scaling factor** ( $F$ ) and **crossover probability** ( $CR$ ): control mutation amplitude and recombination rate, respectively.
- **GT parameters** ( $\mu, \sigma$ ): mean and standard deviation of the Gaussian perturbation. In most cases,  $\mu = \mathbf{0}$  is used, while  $\sigma$  controls the exploration radius.
- **SHIO success-history parameter** ( $SH$ ): controls the influence of historical success information (as defined by SHIO) on the refinement dynamics.

### 3.3 Algorithmic workflow

SHIODEG proceeds through four main phases:

1. **Initialization:** sample an initial population uniformly within the box constraints.
2. **DE variation with GT perturbation:** generate trial candidates via DE mutation/crossover and inject Gaussian perturbations to sustain diversity.
3. **SHIO refinement:** update candidates using leader-based SHIO dynamics (best three solutions) with a time-varying control parameter to transition from exploration to exploitation.
4. **Selection and termination:** apply greedy selection (minimization) and stop at  $L_{\max}$  (or another criterion); return the best solution found.

### 3.4 Mathematical formulation

We consider the bound-constrained minimization problem:

$$\min_{\mathbf{x} \in \mathbb{R}^D} f(\mathbf{x}) \quad \text{s.t.} \quad lb_j \leq x_j \leq ub_j, \quad j = 1, \dots, D. \quad (1)$$

Let  $\mathbf{X}_i^l = [x_{i1}^l, \dots, x_{iD}^l]^\top$  denote candidate  $i$  at iteration  $l$ .

#### 3.4.1 Notation and symbols

Table 2 provides a comprehensive summary of the control parameters used in SHIODEG and the notation adopted in this study.

#### 3.4.2 1) Initialization

Each coordinate is sampled uniformly within the bounds (Table 2):

$$x_{ij}^0 = lb_j + \text{rand}_{ij}(ub_j - lb_j), \quad i = 1, \dots, N, \quad j = 1, \dots, D. \quad (2)$$

Fitness values are computed as:

$$f_i^0 = f(\mathbf{X}_i^0), \quad i = 1, \dots, N. \quad (3)$$

**Table 2** Notation and control parameters used in SHIODEG

Symbol	Meaning
$N$	Population size
$D$	Problem dimension
$l$	Iteration index, $l = 0, 1, \dots, L_{\max}$
$L_{\max}$	Maximum number of iterations
$\mathbf{lb}, \mathbf{ub}$	Bound vectors $\mathbf{lb} = [lb_1, \dots, lb_D]^T$ , $\mathbf{ub} = [ub_1, \dots, ub_D]^T$
$f(\cdot)$	Objective (fitness) function
rand()	Uniform random number in $[0, 1]$
rand <sub>ij</sub>	Independent uniform random number in $[0, 1]$
$F$	DE scaling factor
$CR$	DE crossover probability
$j_{\text{rand}}$	Random dimension index (enforces at least one crossover)
$\mu, \sigma$	Mean and standard deviation of Gaussian perturbation
$\epsilon \sim \mathcal{N}(\mathbf{0}, \mathbf{I}_D)$	Standard $D$ -dimensional Gaussian noise vector
$a(l)$	SHIO control parameter (decreasing schedule)
$\odot$	Hadamard (element-wise) product
$ \cdot $	Element-wise absolute value (for vectors)

### 3.4.3 2) DE Variation with Gaussian Perturbation (GT)

For each target vector  $\mathbf{X}_i^l$ , choose three distinct indices  $r_1, r_2, r_3 \in \{1, \dots, N\}$  such that  $r_1 \neq r_2 \neq r_3 \neq i$ .

Mutation (DE/rand/1) with GT.

$$\mathbf{V}_i^l = \mathbf{X}_{r_1}^l + F(\mathbf{X}_{r_2}^l - \mathbf{X}_{r_3}^l) + \mu + \sigma \epsilon_i^l, \quad \epsilon_i^l \sim \mathcal{N}(\mathbf{0}, \mathbf{I}_D). \tag{4}$$

Setting  $\sigma = 0$  recovers the standard DE/rand/1 mutation. The GT term provides an explicit stochastic exploration component controlled by  $\sigma$  (and centered by  $\mu$ ).

Binomial crossover. A trial vector  $\mathbf{U}_i^l = [u_{i1}^l, \dots, u_{iD}^l]^T$  is produced as:

$$u_{ij}^l = \begin{cases} v_{ij}^l, & \text{if rand}_{ij} \leq CR \text{ or } j = j_{\text{rand}}, \\ x_{ij}^l, & \text{otherwise,} \end{cases} \quad j = 1, \dots, D. \tag{5}$$

Boundary handling. After variation steps, feasibility is enforced by clipping:

$$x_{ij} \leftarrow \min(\max(x_{ij}, lb_j), ub_j), \quad i = 1, \dots, N, j = 1, \dots, D. \tag{6}$$

Selection (minimization).

$$\mathbf{X}_i^{l,DE} = \begin{cases} \mathbf{U}_i^l, & \text{if } f(\mathbf{U}_i^l) < f(\mathbf{X}_i^l), \\ \mathbf{X}_i^l, & \text{otherwise.} \end{cases} \tag{7}$$

### 3.4.4 3) SHIO Refinement Stage

Let  $\mathcal{P}^{l,DE} = \{\mathbf{X}_i^{l,DE}\}_{i=1}^N$ . Denote the best three solutions (by fitness) in  $\mathcal{P}^{l,DE}$  as  $\mathbf{X}_{(1)}^l, \mathbf{X}_{(2)}^l, \mathbf{X}_{(3)}^l$ .

Control parameter schedule.

$$a(l) = 2 \left( 1 - \frac{l}{L_{\max}} \right). \tag{8}$$

Leader-driven update. To avoid ambiguity and emphasize the averaging structure, define three intermediate vectors:

$$\mathbf{Y}_{i,1}^l = \mathbf{X}_{(1)}^l + \mathbf{A}_i^l \odot |\mathbf{X}_{(1)}^l - \mathbf{X}_i^{l,DE}|, \tag{9}$$

$$\mathbf{Y}_{i,2}^l = \mathbf{X}_{(2)}^l, \quad \mathbf{Y}_{i,3}^l = \mathbf{X}_{(3)}^l, \tag{10}$$

where  $\mathbf{A}_i^l = 2a(l)\mathbf{r}_i^l - a(l)$  and  $\mathbf{r}_i^l \in [0, 1]^D$  is a vector of independent uniform random numbers. The SHIO refinement update is then:

$$\mathbf{X}_i^{l+1} = \frac{1}{3} \left( \mathbf{Y}_{i,1}^l + \mathbf{Y}_{i,2}^l + \mathbf{Y}_{i,3}^l \right). \tag{11}$$

Boundary handling in Eq. (6) is applied to  $\mathbf{X}_i^{l+1}$ .

Fitness evaluation and best tracking.

$$f_i^{l+1} = f(\mathbf{X}_i^{l+1}), \quad i = 1, \dots, N. \tag{12}$$

The best solution is tracked via:

$$i^*(l) = \arg \min_{1 \leq i \leq N} f(\mathbf{X}_i^l), \quad \mathbf{X}_{\text{best}}^l = \mathbf{X}_{i^*(l)}^l. \tag{13}$$

Optionally, a convergence curve can be stored as  $\text{Convergence\_curve}(l) = f(\mathbf{X}_{\text{best}}^l)$ .

### 3.4.5 4) Termination

The procedure terminates when  $l = L_{\max}$  (or another stopping rule is met) and returns  $\mathbf{X}_{\text{best}}^{L_{\max}}$ .

## 3.5 Pseudocode

Algorithm 1 provides an equation-traceable implementation of SHIODEG, where each operator call is explicitly linked to its mathematical definition. The procedure starts by sampling an initial population uniformly within the box constraints using Eq. (2) and evaluating all fitness values using Eq. (3). The current best solution  $\mathbf{X}_{\text{best}}^0$  is then identified via Eq. (13).

At each iteration  $l = 0, \dots, L_{\max} - 1$ , SHIODEG executes two sequential stages. In the first stage (DE+GT), each target vector  $\mathbf{X}_i^l$  generates a mutant vector  $\mathbf{V}_i^l$  using

the DE/rand/1 mutation augmented with Gaussian perturbation (Eq. (4)). A trial vector  $\mathbf{U}_i^l$  is then formed through binomial crossover (Eq. (5)), followed by feasibility enforcement through clipping to  $[\mathbf{lb}, \mathbf{ub}]$  (Eq. (6)). A greedy selection step (Eq. (7)) produces an intermediate population  $\mathcal{P}^{l,DE} = \{\mathbf{X}_i^{l,DE}\}_{i=1}^N$ , which retains only improving candidates under minimization.

In the second stage (SHIO refinement), the top three leaders  $\mathbf{X}_{(1)}^l, \mathbf{X}_{(2)}^l, \mathbf{X}_{(3)}^l$  are extracted from  $\mathcal{P}^{l,DE}$  based on fitness ranking. The time-varying control parameter  $a(l)$  is updated according to Eq. (8), which gradually reduces randomness over time. Each candidate is then refined by constructing the leader-driven intermediate vectors  $\mathbf{Y}_{i,1}^l, \mathbf{Y}_{i,2}^l, \mathbf{Y}_{i,3}^l$  via Eqs. (9)–(10), and averaging them to obtain the next iterate  $\mathbf{X}_i^{l+1}$  (Eq. (11)). Boundary handling (Eq. (6)) is reapplied to preserve feasibility. Finally, all solutions are evaluated (Eq. (12)), and the global best  $\mathbf{X}_{\text{best}}^{l+1}$  is updated using Eq. (13). After reaching  $L_{\text{max}}$  iterations, the algorithm returns  $\mathbf{X}_{\text{best}}^{L_{\text{max}}}$  as the final output (optionally with a stored convergence curve).

**Algorithm 1** SHIODEG Optimizer (Equation-Referenced)

---

```

1: Input:  $N, D$ , bounds  $\mathbf{lb}, \mathbf{ub}$ ,  $L_{\text{max}}$ ,  $(F, CR, \mu, \sigma)$ , objective  $f(\cdot)$ .
2: Output:  $\mathbf{X}_{\text{best}}^{L_{\text{max}}}$  (and optionally Convergence_curve).
3: Initialize  $\mathbf{X}_i^0$  using Eq. (2); evaluate  $f_i^0$  using Eq. (3).
4: Determine  $\mathbf{X}_{\text{best}}^0$  using Eq. (13).
5: for  $l = 0$  to  $L_{\text{max}} - 1$  do
6:   DE+GT stage:
7:   for  $i = 1$  to  $N$  do
8:     Select distinct  $r_1, r_2, r_3 \in \{1, \dots, N\} \setminus \{i\}$ .
9:     Compute mutant  $\mathbf{V}_i^l$  using Eq. (4).
10:    Sample  $j_{\text{rand}} \in \{1, \dots, D\}$  and compute trial  $\mathbf{U}_i^l$  using Eq. (5).
11:    Apply bounds to  $\mathbf{U}_i^l$  using Eq. (6).
12:    Apply DE selection to obtain  $\mathbf{X}_i^{l,DE}$  using Eq. (7).
13:   end for
14:   SHIO refinement stage:
15:   Identify leaders  $\mathbf{X}_{(1)}^l, \mathbf{X}_{(2)}^l, \mathbf{X}_{(3)}^l$  from  $\{\mathbf{X}_i^{l,DE}\}_{i=1}^N$ .
16:   Compute  $a(l)$  using Eq. (8).
17:   for  $i = 1$  to  $N$  do
18:     Compute  $\mathbf{Y}_{i,1}^l, \mathbf{Y}_{i,2}^l, \mathbf{Y}_{i,3}^l$  using Eqs. (9)–(10).
19:     Update  $\mathbf{X}_i^{l+1}$  using Eq. (11) and apply Eq. (6).
20:   end for
21:   Evaluate  $f_i^{l+1}$  using Eq. (12).
22:   Update  $\mathbf{X}_{\text{best}}^{l+1}$  using Eq. (13).
23: end for
24: return  $\mathbf{X}_{\text{best}}^{L_{\text{max}}}$ .

```

---

### 3.6 Exploration–exploitation discussion

SHIODEG balances exploration and exploitation through complementary mechanisms. DE mutation generates difference-based steps whose magnitude adapts to population spread, while the GT perturbation adds an explicit stochastic component that prevents step collapse when the population contracts. The greedy DE selection introduces exploitation pressure by accepting only improving trials (for minimization), and the SHIO refinement stage intensifies search around the best three leaders. The SHIO control parameter  $a(l)$  in Eq. (8) decreases over iterations, yielding a gradual transition from exploration to exploitation.

## 4 Validation

All experiments were conducted in MATLAB on a machine equipped with an Intel Core i7 CPU and 32 GB RAM. Each benchmark function was executed 30 independent runs, and the results were reported using mean, standard deviation, and standard error of the mean (SEM). Unless stated otherwise, the population size was fixed to  $N = 100$ , and the maximum number of function evaluations was set to  $1000 \times D$ .

### 4.1 Benchmark functions and validation

The 2022 IEEE Congress on Evolutionary Computation (CEC2022) benchmark functions are used to evaluate and compare the performance of optimization algorithms across a wide range of challenges, encompassing different types of landscapes and complexities. These functions are divided into various categories, including unimodal, simple multimodal, hybrid, and composition functions, each presenting unique characteristics such as smooth, deceptive, and rugged surfaces. The unimodal functions typically have a single global optimum, making them ideal for testing the exploitation capabilities of algorithms. In contrast, the simple multimodal functions contain multiple local optima, challenging an algorithm's ability to avoid premature convergence. Hybrid functions combine multiple basic functions to create complex landscapes, testing both exploration and exploitation, while Composition functions blend several global and local structures, further increasing the complexity and difficulty of optimization. The CEC2022 functions are formulated to provide a comprehensive testbed that reflects real-world optimization problems, ensuring that the performance of algorithms can be robustly assessed under various conditions.

### 4.2 Compared optimizers

To ensure a fair and transparent assessment of the proposed method, this study benchmarks it against a diverse set of state-of-the-art metaheuristic optimizers that represent different search paradigms and update mechanisms (e.g., swarm

intelligence, evolutionary operators, and physics-/behavior-inspired rules). All competitors are executed under the same experimental protocol (identical population size, termination budget, bounds, and constraint-handling policy), so that any performance differences can be attributed to the intrinsic search behavior of each algorithm rather than to unequal settings. Tables 3 and 4 summarize the compared optimizers, reporting their full names, original publication years, and the main control parameters used in our implementations; the citations in the second column point to the original algorithm descriptions.

### 4.3 Results

In the comparative analysis of SHIODEG against other optimizers on the CEC2022 benchmark functions, SHIODEG consistently demonstrates superior performance across multiple functions. For Function F1, SHIODEG achieves the best mean value, ranking first among all optimizers, which underscores its superior performance and stability. This is further evidenced by its lowest standard error of the mean (SEM) and minimal standard deviation (STD), highlighting SHIODEG's consistency as an optimizer. In Function F2, SHIODEG once again secures the top rank, showcasing its robustness and reliability in navigating diverse optimization landscapes. Although the performance gap slightly narrows in Function F3, SHIODEG still maintains a strong position, ranking second. Collectively, these results affirm SHIODEG's effectiveness and reliability, outperforming a range of both traditional and modern metaheuristic optimizers, including FLO, STOA, and FVIM, which exhibit higher error margins, greater variability, and lower rankings. SHIODEG thus emerges as particularly well-suited for tackling challenging optimization problems.

Expanding on SHIODEG's performance across the CEC2022 benchmark functions, the results consistently highlight its superiority and stability in comparison with other optimizers. In Function F4, SHIODEG achieves the lowest mean value and ranks first among all competitors, with minimal error margin (ErrorM), standard deviation (STD), and standard error of the mean (SEM). This suggests a highly reliable and consistent performance, reflected in its ability to deliver robust solutions with minimal variance. SHIODEG continues to excel in Function F5, securing the top position once more, supported by the lowest mean and error metrics, demonstrating its robustness and precision. Although SHIODEG ranks slightly lower in Function F6, it still performs admirably, achieving high accuracy with the lowest error and variability measures among the top optimizers. These outcomes indicate that SHIODEG is highly effective in addressing complex optimization challenges, outperforming a broad spectrum of both traditional and contemporary metaheuristic optimizers such as FLO, STOA, and FVIM, which tend to show higher error margins, greater variability, and lower rankings. Overall, SHIODEG proves to be a strong and consistent competitor across different benchmark functions.

When evaluated against other optimizers on the CEC2022 benchmark functions F7, F8, and F9, SHIODEG continues to exhibit strong performance. In Function F7, SHIODEG ranks first, achieving the lowest mean value among all competitors, which underscores its superior optimization capabilities. The low error margin

**Table 3** Compared optimizers metaheuristic optimization algorithms part 1

Algo.	Full name	Year	Main parameters (controls)
SHIO	Success-History Intelligent Optimizer [54]	2021	Population size; memory of top 3 solutions guiding
FLO	Fritted Lizard Optimization [55]	2024	Population size; two-phase hunt (exploration vs. exploitation) with dynamic transition
STOA	Sooty Tern Optimization Algorithm [56]	2019	Population (number of terns); parameters $A$ and $C$ for exploration–exploitation balance
SOA	Seagull Optimization Algorithm [57]	2019	Population size; spiral attack factor $b$ ; linearly decreasing coefficient $a$ for exploration
FVIM	Four Vector Intelligent Metaheuristic [58]	2024	Population size; 4 leader vectors (guiding positions); archive of best solutions
SPBO	Student Psychology Based Optimization [59]	2020	Population size; performance-based grouping of students; learning factor for “top student” influence
AO	Aquila Optimizer [60]	2021	Population size; four hunting strategies (soaring, bounding flight, exploratory dives) with phase transition parameter
SSOA	Shuffled Shepherd Optimization Algorithm [61]	2020	Population divided into herds; number of herds; “shepherd–horse–sheep” roles; no extra tunable parameters (self-adaptive)
TTHHO	Transient Trigonometric Harris Hawks Optimizer [62]	2024	Population size; hybridization weights mixing Trigonometric (TSO), Sine–Cosine (SCA) and HHO phases
Chimp	Chimp Optimization Algorithm [63]	2020	Population size; four chimp roles (driver, chaser, barrier, attacker) proportions; sexual motivation factor in position update
SO	Snake Optimizer [64]	2022	Population size; “temperature” and “food” thresholds for mating; fixed cooling rate for search intensity
CPO	Crested Porcupine Optimizer [65]	2024	Population size; defensive formation radius; quill deployment threshold (no additional control parameters—behavioral)
ROA	Remora Optimization Algorithm [66]	2021	Population size; host–parasite ratio (remoras per host); mimicry factor from Sailfish and Whale algorithms
COA	Coyote Optimization Algorithm [67]	2018	Population size; number of packs; migration rate (coyotes exchange between packs); reproduction rate
GWO	Grey Wolf Optimizer [68]	2014	Pack size (population); encirclement coefficients $a, A, C$ (with $a$ decreasing linearly to 0)
WOA	Whale Optimization Algorithm [69]	2016	Pod size (population); spiral motion parameter $b$ (shape of spiral, often $b=1$ ); $a$ coefficient decreasing from 2 to 0

Table 3 (continued)

Algo.	Full name	Year	Main parameters (controls)
MFO	Moth-Flame Optimizer [70]	2015	Population size (moths); number of flames (leaders) which decreases linearly during iterations; logarithmic spiral flight path factor
ZOA	Zebra Optimization Algorithm [71]	2022	Population size; two main phases (forage vs. defense) with switch triggered by iteration count; no extra tunable constant
MTDE	Multi-Trial Vector Differential Evolution [72]	2020	Base DE parameters (population, $F$ , $CR$ ); multiple trial vector producers (representative, random-local, global-history) for each subpopulation

**Table 4** Compared optimizers metaheuristic optimization algorithms part 2

Algo.	Full name	Year	Main parameters (controls)
SCA	Sine Cosine Algorithm [73]	2016	Population size; oscillation amplitude $r$ (linearly decreasing from $\alpha$ to 0) controlling sine/cosine term range
DOA	Dandelion Optimizer Algorithm [74]	2022	Population size; seed dispersal count; wind dispersion factor (implicit in update equations, not user-set)
HHO	Harris Hawks Optimization [75]	2019	Population size; escape energy $E_0$ (initially $E_0=2$ , decreases to 0); random jump strength $q$ (stochastic, no fixed parameter)
SCSO	Sand Cat Swarm Optimization [76]	2022	Population size; night-time hunting mode (implicit, no parameter); high sensitivity to prey sound frequency (no explicit parameter, behaviorally modeled)
GA	Genetic Algorithm [77]	1975	Population size; crossover probability; mutation probability (plus encoding of solutions and selection scheme)
SA	Simulated Annealing [78]	1983	Initial temperature $T_0$ ; cooling schedule (rate of temperature reduction); equilibrium iterations per temperature
AVOA	African Vultures Optimization Algorithm [79]	2021	Population size; exploitation weight $W$ (fraction of vultures tracking best vs. second-best prey); spiral flight angle in navigation (fixed formula)
BBO	Biogeography-Based Optimization [80]	2008	Population (habitat count); immigration rate $\lambda$ and emigration rate $\mu$ (per habitat, typically linear with habitat suitability rank); mutation rate
RIME	Rime Optimization Algorithm [81]	2023	Population size; rime-ice growth factor (simulating deposition of ice, intrinsic to update equations); no external parameters besides DE-like crossover rate in variants
FOX	Fox Optimization Algorithm [82]	2023	Population size; leap strength (distance scaling for fox's jump, adaptively set by distance to prey); randomness in jump direction (inherent in algorithm)
OHO	Oriole (Oriole) Heuristic Optimization [83]	2025	Population size; dual-scale foraging ratio (macroscopic vs. microscopic search balance); vocal communication frequency (how often solutions share info)

(ErrorM), standard deviation (STD), and standard error of the mean (SEM) further reinforce its robustness and reliability. In Function F8, SHIODEG maintains its leading position by securing the top rank, demonstrating its effectiveness across various optimization landscapes. Although there is some increase in variability compared to the top-performing optimizers in Function F9, SHIODEG still ranks third, outperforming the majority of the other optimizers. The consistent rankings across these functions indicate that SHIODEG is a reliable and highly effective optimizer, capable of handling complex optimization problems with greater stability and accuracy than many of its competitors.

Finally, in comparing SHIODEG with other optimizers over the CEC2022 benchmark functions F10, F11, and F12, SHIODEG once again showcases its superior performance. In Function F10, SHIODEG ranks first, achieving the lowest mean value, indicative of its strong optimization capabilities. The low standard deviation (STD) and standard error of the mean (SEM) further emphasize its stability and consistency. SHIODEG continues to lead in Function F11, ranking first again with the best mean value among all optimizers, which highlights its robustness across varying optimization landscapes. Although SHIODEG ranks second in Function F12, it still performs remarkably well, with competitive performance and low variability as evidenced by the STD and SEM values. These results collectively illustrate that SHIODEG is a highly effective and reliable optimizer, consistently outperforming many other metaheuristic algorithms across a wide range of challenging benchmark functions (See Tables 5, 6, 7).

#### 4.3.1 Wilcoxon sum-rank test results

The Wilcoxon sum-rank test results reveal that the SHIODEG optimizer has outperformed other optimizers in a consistent and significant manner. With a total of 12 wins and no losses or ties across all benchmark functions, SHIODEG demonstrates superior performance. This is comparable to other top-performing optimizers such as FLO, SPBO, AO, SSOA, TTHHO, Chimp, WOA, MTDE, SCSO, GA, and OHO, which also achieved a flawless record of 12 wins with no losses or ties. However, it surpasses algorithms like SO, MFO, ZOA, SA, and others that recorded a few losses or ties, indicating that SHIODEG not only maintains a strong competitive edge but also excels across diverse optimization problems. This consistent dominance underscores the robustness and reliability of SHIODEG in solving complex optimization tasks. Moreover, because metaheuristic optimizers are stochastic, each algorithm was executed for  $R$  independent runs per function. The resulting distributions of final objective values are frequently non-normal (skewed/heavy-tailed) and may contain outliers on multimodal/hybrid/composition functions. Therefore, instead of using the paired  $t$ -test (which assumes approximate normality of paired differences), we employ the Wilcoxon signed-rank test, a nonparametric paired alternative that compares the median of paired differences via ranks and requires weaker assumptions. This choice follows established recommendations for comparing evolutionary and swarm intelligence algorithms [84–86].

For each benchmark function, we form paired samples by aligning run indices (using the same experimental protocol and matched random-seed setting across

algorithms). The null hypothesis is that the median of the pairwise performance differences between SHIODEG and a competitor is zero. We report the corresponding  $p$ -values and determine significance at  $\alpha = 0.05$ . As reported in Tables 14, 15 and 16. Since multiple pairwise comparisons are performed, we additionally apply a multiple-comparison correction (Holm) to control the family-wise error rate [84, 85].

Across CEC2022 functions F1–F12 (see Figs. 1 and 2), the *search history* panels show that SHIODEGT begins with wide, problem-scale exploration and then progressively contracts its sampling toward compact regions, indicating a successful transition from global scouting to local refinement for most cases. For relatively well-behaved landscapes (e.g., F1, F3, F4, F8, F10, and F12), the clouds of visited points rapidly collapse into a tight cluster around the best basin, with only sparse outliers remaining from early exploration. In contrast, more rugged or composite landscapes (notably F2, F6, F9, and F11) exhibit multi-cluster or elongated point patterns, reflecting competing attraction regions and basin switching before commitment. This behavior is consistent with the *trajectory* plots, where all population settings exhibit a short transient with large oscillations in the first iterations (exploration bursts and corrective moves), followed by near-stationary dynamics around the best region (exploitation). The harder functions preserve mild oscillations or biased drifts for longer (e.g., F2/F5/F6/F9), which suggests that SHIODEGT continues probing to escape local traps rather than collapsing prematurely.

The average fitness curves further confirm this two-stage behavior: for several functions (e.g., F1, F3, F9, F11, and F12), the mean fitness drops by multiple orders of magnitude within the first few dozen iterations and then stabilizes, indicating fast basin identification and consistent population-wide improvement. For the more challenging cases (e.g., F2, F4, F5, F7, F8, and F10), the decline is slower and frequently exhibits extended plateaus, implying that a portion of the population remains distributed across suboptimal basins while the best region is refined gradually. Importantly, population size modulates this dynamic: larger populations tend to maintain broader coverage early on (often yielding smoother mean trends and improved stability), while smaller populations can show sharper early drops but also higher susceptibility to stagnation on difficult landscapes. The medium-sized population frequently provides a strong compromise, sustaining enough diversity to avoid early trapping while still concentrating search pressure effectively once a promising basin is detected.

The convergence (best-so-far) curves exhibit a characteristic staircase profile across many functions, with rapid early gains followed by discrete improvements separated by plateaus, a typical signature of alternating intensification and successful escape/restart events. On functions where SHIODEGT identifies the global basin quickly (e.g., F1, F3, F9, F11, and F12), convergence is steep and stabilizes early, showing that the optimizer reaches high-quality solutions within a relatively small fraction of the iteration budget. Conversely, for functions with stronger multimodality/composition effects (e.g., F2, F4, F5, F7, F8, and F10), the best fitness improves more gradually and remains sensitive to population size, with different  $N \in \{30, 50, 100\}$  achieving different trade-offs between speed (early descent) and end quality (late-stage improvements). Overall, the combined evidence from

Table 5 Results on IEEE Congress on Evolutionary Computation (CEC) 2022 Benchmark suit

Function	Measure	SHIODEG	SHIO	DE	FLO	STOA	SOA	FVIM	SPBO	AO	SSOA	TTHHO
F1	Mean	3.000E+02	3.877E+03	1.846E+03	8.232E+03	1.557E+03	1.550E+03	4.685E+03	3.006E+04	8.630E+02	1.171E+04	3.138E+02
	ErrorM	6.012E-03	3.577E+03	1.546E+03	7.932E+03	1.257E+03	1.250E+03	4.385E+03	2.976E+04	5.630E+02	1.141E+04	1.380E+01
	STD	2.653E-03	3.211E+03	7.343E+02	1.457E+03	1.373E+03	1.651E+03	3.028E+03	5.277E+03	4.400E+02	3.566E+03	2.604E+01
	SEM	4.843E-04	5.862E+02	3.284E+02	2.660E+02	2.507E+02	3.015E+02	5.529E+02	9.634E+02	8.033E+01	6.510E+02	4.755E+00
	Rank	1	21	18	25	16	15	22	31	13	27	8
F2	Mean	4.047E+02	4.300E+02	4.055E+02	1.342E+03	4.310E+02	4.604E+02	4.253E+02	1.148E+03	4.228E+02	1.507E+03	4.618E+02
	ErrorM	5.693E+00	2.995E+01	5.527E+00	9.419E+02	3.098E+01	6.038E+01	2.527E+01	7.476E+02	2.278E+01	1.107E+03	6.179E+01
	STD	2.853E+00	2.726E+01	1.234E+00	4.541E+02	2.552E+01	9.328E+01	2.488E+01	2.049E+02	4.552E+01	5.000E+02	7.893E+01
	SEM	5.208E-01	4.977E+00	5.520E-01	8.291E+01	4.660E+00	1.703E+01	4.543E+00	3.740E+01	8.312E+00	9.129E+01	1.441E+01
	Rank	1	18	2	30	19	22	15	29	14	31	24
F3	Mean	6.000E+02	6.055E+02	6.001E+02	6.469E+02	6.109E+02	6.104E+02	6.033E+02	6.703E+02	6.135E+02	6.562E+02	6.369E+02
	ErrorM	4.226E-02	5.492E+00	5.316E-02	4.687E+01	1.092E+01	1.038E+01	3.295E+00	7.030E+01	1.349E+01	5.624E+01	3.692E+01
	STD	1.053E-02	4.078E+00	5.68434E-14	9.806E+00	4.802E+00	5.305E+00	4.853E+00	8.506E+00	5.948E+00	9.590E+00	1.194E+01
	SEM	1.922E-03	7.445E-01	2.54211E-14	1.790E+00	8.767E-01	9.686E-01	8.861E-01	1.553E+00	1.086E+00	1.751E+00	2.179E+00
	Rank	2	9	3	27	13	12	7	32	15	29	25
F4	Mean	8.136E+02	8.163E+02	8.172E+02	8.528E+02	8.220E+02	8.259E+02	8.138E+02	8.980E+02	8.181E+02	8.605E+02	8.275E+02
	ErrorM	1.363E+01	1.634E+01	1.722E+01	5.283E+01	2.204E+01	2.587E+01	1.357E+01	9.796E+01	1.807E+01	6.046E+01	2.753E+01
	STD	9.260E+00	9.190E+00	2.757E+00	9.843E+00	7.727E+00	8.328E+00	6.604E+00	1.161E+01	8.925E+00	1.072E+01	6.163E+00
	SEM	1.691E+00	1.678E+00	1.233E+00	1.797E+00	1.411E+00	1.520E+00	1.206E+00	2.120E+00	1.629E+00	1.957E+00	1.125E+00
	Rank	1	5	8	28	10	13	2	32	9	29	16
F5	Mean	9.000E+02	9.617E+02	9.001E+02	1.387E+03	9.607E+02	9.876E+02	9.166E+02	3.767E+03	1.006E+03	1.618E+03	1.362E+03
	ErrorM	1.016E-03	6.170E+01	1.068E-01	4.874E+02	6.074E+01	8.759E+01	1.661E+01	2.867E+03	1.057E+02	7.184E+02	4.615E+02
	STD	4.071E-04	1.119E+02	5.516E-02	1.613E+02	3.749E+01	8.401E+01	2.216E+01	6.212E+02	6.594E+01	1.979E+02	2.022E+02
	SEM	7.433E-05	2.042E+01	2.467E-02	2.945E+01	6.844E+00	1.534E+01	4.047E+00	1.134E+02	1.204E+01	3.612E+01	3.692E+01
	Rank	1	9	2	23	8	10	5	32	15	30	22

Table 5 (continued)

Function	Measure	SHIODEG	SHIO	DE	FLO	STOA	SOA	FVIM	SPBO	AO	SSOA	TTHHO
F6	Mean	1.928E+03	3.718E+03	2.353E+03	3.698E+07	1.890E+04	1.898E+04	3.801E+03	3.439E+08	1.040E+04	1.663E+08	4.597E+03
	ErrorM	1.280E+02	1.918E+03	5.531E+02	3.697E+07	1.710E+04	1.718E+04	2.001E+03	3.439E+08	8.604E+03	1.663E+08	2.797E+03
	STD	4.911E+01	1.425E+03	3.068E+02	3.942E+07	9.718E+03	1.088E+04	2.047E+03	2.916E+08	5.779E+03	1.720E+08	2.294E+03
	SEM	8.966E+00	2.602E+02	1.372E+02	7.196E+06	1.774E+03	1.987E+03	3.736E+02	5.325E+07	1.055E+03	3.140E+07	4.188E+02
	Rank	1	10	2	29	21	22	11	31	20	30	17
F7	Mean	2.003E+03	2.048E+03	2.004E+03	2.101E+03	2.034E+03	2.035E+03	2.044E+03	2.163E+03	2.045E+03	2.136E+03	2.071E+03
	ErrorM	3.349E+00	4.806E+01	4.475E+00	1.008E+02	3.436E+01	3.542E+01	4.446E+01	1.633E+02	4.458E+01	1.355E+02	7.129E+01
	STD	6.876E+00	2.304E+01	2.997E-01	2.334E+01	1.205E+01	9.267E+00	2.189E+01	4.019E+01	1.801E+01	2.548E+01	2.930E+01
	SEM	1.255E+00	4.206E+00	1.340E-01	4.261E+00	2.201E+00	1.692E+00	3.996E+00	7.337E+00	3.287E+00	4.652E+00	5.350E+00
	Rank	1	17	2	26	10	11	14	32	15	31	23
F8	Mean	2.204E+03	2.228E+03	2.210E+03	2.243E+03	2.227E+03	2.228E+03	2.224E+03	2.353E+03	2.229E+03	2.367E+03	2.232E+03
	ErrorM	4.279E+00	2.823E+01	1.040E+01	4.303E+01	2.687E+01	2.797E+01	2.426E+01	1.527E+02	2.856E+01	1.674E+02	3.190E+01
	STD	6.086E+00	4.968E+00	2.845E+00	1.571E+01	5.429E+00	3.338E+00	4.172E+00	1.008E+02	4.048E+00	9.826E+01	1.185E+01
	SEM	1.111E+00	9.070E-01	1.273E+00	2.869E+00	9.911E-01	6.095E-01	7.618E-01	1.841E+01	7.391E-01	1.794E+01	2.164E+00
	Rank	1	16	2	24	12	15	8	29	17	30	18
F9	Mean	2.529E+03	2.599E+03	2.530E+03	2.745E+03	2.570E+03	2.578E+03	2.582E+03	2.737E+03	2.563E+03	2.794E+03	2.585E+03
	ErrorM	2.293E+02	2.995E+02	2.298E+02	4.446E+02	2.697E+02	2.776E+02	2.819E+02	4.368E+02	2.631E+02	4.940E+02	2.854E+02
	STD	4.933E-05	4.284E+01	3.236E-08	3.886E+01	4.077E+01	3.783E+01	3.693E+01	6.730E+01	2.609E+01	4.095E+01	4.764E+01
	SEM	9.007E-06	7.822E+00	1.447E-08	7.094E+00	7.443E+00	6.907E+00	6.742E+00	1.229E+01	4.764E+00	7.477E+00	8.698E+00
	Rank	3	25	4	30	18	21	22	29	17	31	23
F10	Mean	2.504E+03	2.580E+03	2.506E+03	2.671E+03	2.505E+03	2.505E+03	2.568E+03	2.577E+03	2.565E+03	2.727E+03	2.578E+03
	ErrorM	1.037E+02	1.798E+02	1.057E+02	2.706E+02	1.047E+02	1.046E+02	1.675E+02	1.773E+02	1.652E+02	3.271E+02	1.784E+02
	STD	1.922E+01	7.108E+01	1.368E-01	1.326E+02	2.223E+01	2.141E+01	5.586E+01	3.957E+01	6.144E+01	1.276E+02	8.913E+01
	SEM	3.508E+00	1.298E+01	6.120E-02	2.421E+01	4.058E+00	3.909E+00	1.020E+01	7.224E+00	1.122E+01	2.330E+01	1.627E+01
	Rank	1	22	5	26	3	2	19	20	16	29	21

Table 5 (continued)

Function	Measure	SHIODEG	SHIO	DE	FLO	STOA	SOA	FVIM	SPBO	AO	SSOA	TTHO
F11	Mean	2.611E+03	2.806E+03	2.647E+03	3.614E+03	2.830E+03	2.798E+03	2.850E+03	3.712E+03	2.732E+03	3.569E+03	2.818E+03
	ErrorM	1.055E+01	2.057E+02	4.742E+01	1.014E+03	2.302E+02	1.985E+02	2.501E+02	1.112E+02	1.318E+03	9.692E+02	2.180E+02
	STD	3.802E+01	1.541E+02	3.212E+01	4.323E+02	1.824E+02	1.598E+02	2.230E+02	4.348E+02	1.465E+02	3.610E+02	1.967E+02
	SEM	6.942E+00	2.814E+01	1.436E+01	7.893E+01	3.331E+01	2.917E+01	4.072E+01	7.938E+01	2.674E+01	6.592E+01	3.591E+01
	Rank	1	18	2	30	22	15	23	31	6	29	20
F12	Mean	2.863E+03	2.884E+03	2.864E+03	3.053E+03	2.864E+03	2.864E+03	2.883E+03	2.885E+03	2.867E+03	3.053E+03	2.897E+03
	ErrorM	1.633E+02	1.840E+02	1.643E+02	3.533E+02	1.637E+02	1.641E+02	1.832E+02	1.846E+02	1.673E+02	3.525E+02	1.967E+02
	STD	1.667E+00	2.316E+01	8.449E-01	8.030E+01	1.400E+01	1.293E+00	2.274E+01	6.804E+00	2.339E+00	5.564E+01	3.406E+01
	SEM	3.043E-01	4.228E+00	3.779E-01	1.466E+01	2.556E-01	2.360E-01	4.152E+00	1.242E+00	4.271E-01	1.016E+01	6.219E+00
	Rank	2	18	8	31	4	6	17	19	12	30	23

**Table 6** Results on IEEE Congress on Evolutionary Computation (CEC) 2022 Benchmark suit

Function	Measure	Chimp	SO	CPO	ROA	COA	GWO	WOA	MFO	ZOA	MITDE	SCA
F1	Mean	2.009E+03	3.066E+02	7.763E+02	6.826E+03	3.150E+02	1.845E+03	1.678E+04	5.083E+04	7.001E+02	1.694E+04	1.352E+03
	ErrorM	1.709E+03	6.643E+00	4.763E+02	6.526E+03	1.499E+01	1.545E+03	1.648E+04	4.783E+03	4.001E+02	1.664E+04	1.052E+03
	STD	1.064E+03	9.184E+00	8.588E+02	2.389E+03	4.612E+01	1.728E+03	6.783E+03	5.885E+03	8.863E+02	6.009E+03	4.726E+02
	SEM	1.943E+02	1.677E+00	1.568E+02	4.362E+02	8.421E+00	3.155E+02	1.238E+03	1.075E+03	1.618E+02	1.097E+03	8.629E+01
	Rank	19	7	12	24	9	17	29	23	11	30	14
F2	Mean	6.146E+02	4.149E+02	4.259E+02	6.980E+02	4.099E+02	4.255E+02	4.227E+02	4.129E+02	4.469E+02	5.368E+02	4.616E+02
	ErrorM	2.146E+02	1.495E+01	2.592E+01	2.980E+02	9.944E+00	2.547E+01	2.272E+01	1.286E+01	4.689E+01	1.368E+02	6.158E+01
	STD	1.458E+02	1.981E+01	3.252E+01	1.898E+02	1.782E+01	2.428E+01	2.576E+01	1.430E+01	4.560E+01	4.638E+01	1.636E+01
	SEM	2.662E+01	3.617E+00	5.937E+00	3.465E+01	3.253E+00	4.433E+00	4.703E+00	2.611E+00	8.326E+00	8.468E+00	2.987E+00
	Rank	26	9	17	27	6	16	13	8	20	25	23
F3	Mean	6.288E+02	6.068E+02	6.453E+02	6.364E+02	6.039E+02	6.007E+02	6.362E+02	6.014E+02	6.148E+02	6.284E+02	6.183E+02
	ErrorM	2.876E+01	6.752E+00	4.528E+01	3.644E+01	3.937E+00	7.208E-01	3.619E+01	1.357E+00	1.485E+01	2.843E+01	1.827E+01
	STD	8.588E+00	8.249E+00	1.258E+01	1.365E+01	6.101E+00	7.536E-01	1.255E+01	1.895E+00	5.337E+00	5.540E+00	4.925E+00
	SEM	1.568E+00	1.506E+00	2.297E+00	2.493E+00	1.114E+00	1.376E-01	2.292E+00	3.461E-01	9.745E-01	1.011E+00	8.992E-01
	Rank	21	10	26	24	8	5	23	6	17	20	18
F4	Mean	8.342E+02	8.170E+02	8.326E+02	8.429E+02	8.272E+02	8.143E+02	8.332E+02	8.302E+02	8.145E+02	8.646E+02	8.394E+02
	ErrorM	3.416E+01	1.702E+01	3.257E+01	4.294E+01	2.725E+01	1.433E+01	3.324E+01	3.016E+01	1.153E+01	6.459E+01	3.940E+01
	STD	5.922E+00	8.540E+00	5.826E+00	7.144E+00	8.008E+00	8.031E+00	1.456E+01	1.097E+01	4.557E+00	9.974E+00	5.712E+00
	SEM	1.081E+00	1.559E+00	1.064E+00	1.304E+00	1.462E+00	1.466E+00	2.658E+00	2.003E+00	8.320E-01	1.821E+00	1.043E+00
	Rank	22	6	20	26	15	3	21	19	4	30	25
F5	Mean	1.261E+03	9.264E+02	1.562E+02	1.346E+03	9.881E+02	9.186E+02	1.556E+03	9.925E+02	9.885E+02	1.511E+03	9.966E+02
	ErrorM	3.607E+02	2.638E+01	6.617E+02	4.463E+02	8.808E+01	1.855E+01	6.562E+02	9.249E+01	8.852E+01	6.111E+02	9.659E+01
	STD	1.928E+02	4.204E+01	2.012E+02	2.215E+02	1.790E+02	4.127E+01	4.544E+02	1.834E+02	6.212E+01	3.221E+02	6.753E+01
	SEM	3.520E+01	7.675E+00	3.673E+01	4.045E+01	3.268E+01	7.535E+00	8.297E+01	3.348E+01	1.134E+01	5.880E+01	1.233E+01
	Rank	19	7	28	21	11	6	27	13	12	26	14

Table 6 (continued)

Function	Measure	Chimp	SO	CPO	ROA	COA	GWO	WOA	MFO	ZOA	MITDE	SCA
F6	Mean	1.144E+06	4.079E+03	3.389E+03	6.632E+05	3.676E+03	5.364E+03	3.365E+03	4.425E+03	3.197E+03	8.000E+06	1.834E+06
	ErrorM	1.142E+06	2.279E+03	1.589E+03	6.614E+05	1.876E+03	3.564E+03	1.565E+03	2.625E+03	1.397E+03	7.998E+06	1.832E+06
	STD	8.332E+05	1.712E+03	1.632E+03	1.802E+06	1.678E+03	2.329E+03	1.567E+03	2.322E+03	1.599E+03	6.791E+06	1.591E+06
	SEM	1.521E+05	3.126E+02	2.980E+02	3.290E+05	3.064E+02	4.253E+02	2.862E+02	4.240E+02	2.919E+02	1.240E+06	2.904E+05
	Rank	25	14	6	24	9	19	5	16	4	27	26
F7	Mean	2.057E+03	2.039E+03	2.119E+03	2.082E+03	2.018E+03	2.029E+03	2.066E+03	2.027E+03	2.041E+03	2.083E+03	2.054E+03
	ErrorM	5.749E+01	3.931E+01	1.190E+02	8.233E+01	1.840E+01	2.853E+01	6.588E+01	2.661E+01	4.094E+01	8.284E+01	5.423E+01
	STD	7.854E+00	1.582E+01	6.992E+01	3.311E+01	6.752E+00	1.364E+01	2.058E+01	1.150E+01	1.507E+01	1.847E+01	6.747E+00
	SEM	1.434E+00	2.889E+00	1.277E+01	6.045E+00	1.233E+00	2.491E+00	3.758E+00	2.100E+00	2.751E+00	3.373E+00	1.232E+00
	Rank	20	12	28	24	4	8	21	6	13	25	19
F8	Mean	2.301E+03	2.225E+03	2.279E+03	2.238E+03	2.221E+03	2.227E+03	2.234E+03	2.225E+03	2.225E+03	2.242E+03	2.233E+03
	ErrorM	1.015E+02	2.474E+01	7.919E+01	3.835E+01	2.149E+01	2.711E+01	3.374E+01	2.498E+01	2.476E+01	4.195E+01	3.281E+01
	STD	5.900E+01	6.652E+00	7.363E+01	1.622E+01	8.781E+00	2.342E+01	8.969E+00	5.155E+00	5.017E+00	7.416E+00	2.974E+00
	SEM	1.077E+01	1.214E+00	1.344E+01	2.962E+00	1.603E+00	4.275E+00	1.637E+00	9.412E-01	9.159E-01	1.354E+00	5.429E-01
	Rank	28	9	27	22	5	13	20	11	10	23	19
F9	Mean	2.571E+03	2.503E+03	2.558E+03	2.697E+03	2.534E+03	2.546E+03	2.563E+03	2.531E+03	2.593E+03	2.639E+03	2.561E+03
	ErrorM	2.714E+02	2.030E+02	2.578E+02	3.970E+02	2.342E+02	2.462E+02	2.625E+02	2.305E+02	2.931E+02	3.386E+02	2.611E+02
	STD	1.757E+01	3.575E+01	4.733E+01	5.755E+01	2.683E+01	3.159E+01	4.026E+01	3.751E+00	3.875E+01	2.458E+01	1.575E+01
	SEM	3.208E+00	6.527E+00	8.642E+00	1.051E+01	4.898E+00	5.768E+00	7.350E+00	6.848E-01	7.075E+00	4.488E+00	2.876E+00
	Rank	19	1	14	27	8	10	16	5	24	26	15
F10	Mean	2.706E+03	2.544E+03	2.802E+03	2.592E+03	2.548E+03	2.560E+03	2.563E+03	2.507E+03	2.517E+03	2.522E+03	2.505E+03
	ErrorM	3.059E+02	1.438E+02	4.023E+02	1.917E+02	1.477E+02	1.603E+02	1.626E+02	1.071E+02	1.166E+02	1.221E+02	1.017E+02
	STD	4.931E+02	5.876E+01	5.174E+02	9.888E+01	5.895E+01	5.713E+01	6.765E+01	2.388E+01	4.114E+01	2.590E+01	6.517E-01
	SEM	9.003E+01	1.073E+01	9.446E+01	1.805E+01	1.076E+01	1.043E+01	1.235E+01	4.359E+00	7.512E+00	4.729E+00	1.190E-01
	Rank	27	12	30	24	13	14	15	6	8	9	4

Table 6 (continued)

Function	Measure	Chimp	SO	CPO	ROA	COA	GWO	WOA	MFO	ZOA	MTDE	SCA
F11	Mean	3.279E+03	2.729E+03	2.826E+03	3.116E+03	2.745E+03	2.790E+03	2.755E+03	2.756E+03	2.812E+03	2.911E+03	2.787E+03
	ErrorM	6.794E+02	1.290E+02	2.259E+02	5.157E+02	1.452E+02	1.900E+02	1.551E+02	1.559E+02	2.116E+02	3.114E+02	1.873E+02
	STD	2.431E+02	1.794E+02	2.157E+02	3.036E+02	1.373E+02	1.745E+02	1.481E+02	1.952E+02	1.840E+02	1.100E+02	8.510E+01
	SEM	4.438E+01	3.275E+01	3.939E+01	5.543E+01	2.507E+01	3.186E+01	2.704E+01	3.564E+01	3.360E+01	2.008E+01	1.554E+01
	Rank	27	5	21	26	7	14	9	11	19	25	13
F12	Mean	2.868E+03	2.859E+03	2.914E+03	2.933E+03	2.865E+03	2.864E+03	2.889E+03	2.863E+03	2.935E+03	2.891E+03	2.869E+03
	ErrorM	1.679E+02	1.587E+02	2.136E+02	2.333E+02	1.655E+02	1.642E+02	1.887E+02	1.633E+02	2.353E+02	1.908E+02	1.694E+02
	STD	6.968E+00	1.948E+01	5.407E+01	7.019E+01	2.245E+00	2.661E+00	3.413E+01	1.696E+00	2.982E+01	8.942E+00	1.509E+00
	SEM	1.272E+00	3.556E+00	9.872E+00	1.282E+01	4.099E-01	4.858E-01	6.232E+00	3.096E-01	5.445E+00	1.633E+00	2.755E-01
	Rank	14	1	25	26	9	7	20	3	27	22	15

Table 7 Results on IEEE Congress on Evolutionary Computation (CEC) 2022 Benchmark suit

Function	Measure	DOA	HHO	SCSO	GA	SA	AVOA	BBO	RIME	FOX	OHO
F1	Mean	2.313E+03	3.016E+02	5.560E+02	3.53E+04	1.06E+04	3.00E+02	3.00E+02	3.00E+02	3.00E+02	1.56E+04
	ErrorM	2.013E+03	1.611E+00	2.560E+02	3.50E+04	1.03E+04	1.40E-01	1.31E-02	3.79E-02	5.7E-02	1.53E+04
	STD	2.190E+03	7.503E-01	4.997E+02	1.187E+04	2.892E+03	7.215E-01	1.150E-02	2.83E-02	3.048E-01	6.229E+03
	SEM	3.998E+02	1.370E-01	9.123E+01	2.168E+03	5.280E+02	1.317E-01	2.099E-03	5.172E-03	5.565E-02	1.137E+03
	Rank	20	6	10	32	26	5	2	3	4	28
F2	Mean	4.535E+02	4.218E+02	4.168E+02	7.540E+02	4.151E+02	4.082E+02	4.057E+02	4.061E+02	4.125E+02	2.804E+03
	ErrorM	5.345E+01	2.184E+01	1.684E+01	3.540E+02	1.512E+01	8.185E+00	1.703E+00	6.095E+00	1.246E+01	2.404E+03
	STD	7.533E+01	2.859E+01	2.256E+01	2.278E+02	5.624E+00	1.317E+01	2.344E+00	3.175E+00	1.975E+01	1.218E+03
	SEM	1.375E+01	5.220E+00	4.118E+00	4.159E+01	1.027E+00	2.404E+00	4.280E-01	5.798E-01	3.606E+00	2.224E+02
	Rank	21	12	11	28	10	5	3	4	7	32
F3	Mean	6.259E+02	6.321E+02	6.139E+02	6.571E+02	6.094E+02	6.117E+02	6.000E+02	6.001E+02	6.517E+02	6.608E+02
	ErrorM	2.594E+01	3.214E+01	1.395E+01	5.714E+01	9.366E+00	1.168E+01	1.845E-03	7.353E-02	5.165E+01	6.081E+01
	STD	1.179E+01	1.130E+01	8.422E+00	1.278E+01	2.365E+00	9.023E+00	1.801E-03	6.477E-02	1.099E+01	3.427E+00
	SEM	2.153E+00	2.063E+00	1.538E+00	2.334E+00	4.317E-01	1.647E+00	3.288E-04	1.183E-02	2.007E+00	6.257E-01
	Rank	19	22	16	30	11	14	1	4	28	31
F4	Mean	8.280E+02	8.236E+02	8.271E+02	8.713E+02	8.379E+02	8.298E+02	8.170E+02	8.227E+02	8.387E+02	8.457E+02
	ErrorM	2.795E+01	2.356E+01	2.709E+01	7.132E+01	3.788E+01	2.980E+01	1.705E+01	2.269E+01	3.870E+01	4.570E+01
	STD	1.020E+01	7.292E+00	8.633E+00	1.387E+01	1.063E+01	1.049E+01	8.199E+00	1.047E+01	1.157E+01	3.965E+00
	SEM	1.863E+00	1.331E+00	1.576E+00	2.531E+00	1.941E+00	1.914E+00	1.497E+00	1.912E+00	2.112E+00	7.240E-01
	Rank	17	12	14	31	23	18	7	11	24	27
F5	Mean	1.083E+03	1.309E+03	1.026E+03	1.390E+03	1.627E+03	1.166E+03	9.055E+02	9.002E+02	1.495E+03	1.613E+03
	ErrorM	1.831E+02	4.091E+02	1.261E+02	4.896E+02	7.266E+02	2.663E+02	5.455E+00	1.963E-01	5.945E+02	7.133E+02
	STD	1.130E+02	1.680E+02	1.244E+02	3.597E+02	3.295E+02	2.156E+02	1.711E+01	3.056E-01	8.222E+01	8.986E+01
	SEM	2.062E+01	3.067E+01	2.271E+01	6.568E+01	6.016E+01	3.936E+01	3.124E+00	5.580E-02	1.501E+01	1.641E+01
	Rank	17	20	16	24	31	18	4	3	25	29

**Table 7** (continued)

Function	Measure	DOA	HHO	SCSO	GA	SA	AVOA	BBO	RIME	FOX	OHO
F6	Mean	2.084E+05	4.083E+03	4.635E+03	3.325E+07	3.925E+03	3.941E+03	2.512E+03	3.627E+03	3.500E+03	8.980E+08
	ErrorM	2.066E+05	2.283E+03	2.835E+03	3.324E+07	2.125E+03	2.141E+03	7.125E+02	1.827E+03	1.700E+03	8.980E+08
	STD	1.128E+06	2.415E+03	1.951E+03	5.055E+07	1.446E+03	2.100E+03	1.053E+03	1.763E+03	1.376E+03	5.736E+08
	SEM	2.060E+05	4.408E+02	3.562E+02	9.230E+06	2.639E+02	3.833E+02	1.923E+02	3.219E+02	2.513E+02	1.047E+08
	Rank	23	15	18	28	12	13	3	8	7	32
F7	Mean	2.052E+03	2.069E+03	2.047E+03	2.111E+03	2.028E+03	2.030E+03	2.021E+03	2.017E+03	2.127E+03	2.121E+03
	ErrorM	5.164E+01	6.865E+01	4.698E+01	1.109E+02	2.778E+01	2.959E+01	2.069E+01	1.650E+01	1.270E+02	1.211E+02
	STD	3.433E+01	3.413E+01	2.012E+01	4.094E+01	4.144E+00	1.048E+01	8.549E+00	2.566E+01	5.545E+01	1.014E+01
	SEM	6.269E+00	6.231E+00	3.673E+00	7.474E+00	7.566E-01	1.914E+00	1.561E+00	4.685E+00	1.012E+01	1.852E+00
	Rank	18	22	16	27	7	9	5	3	30	29
F8	Mean	2.245E+03	2.235E+03	2.227E+03	2.264E+03	2.222E+03	2.224E+03	2.220E+03	2.217E+03	2.402E+03	2.430E+03
	ErrorM	4.500E+01	3.467E+01	2.738E+01	6.433E+01	2.195E+01	2.363E+01	2.037E+01	1.669E+01	2.019E+02	2.298E+02
	STD	4.172E+01	1.387E+01	3.414E+00	4.741E+01	3.125E+00	3.105E+00	8.145E+00	8.068E+00	1.348E+02	1.437E+02
	SEM	7.616E+00	2.533E+00	6.234E-01	8.655E+00	5.705E-01	5.668E-01	1.487E+00	1.473E+00	2.461E+01	2.623E+01
	Rank	25	21	14	26	6	7	4	3	31	32
F9	Mean	2.557E+03	2.558E+03	2.575E+03	2.731E+03	2.533E+03	2.534E+03	2.529E+03	2.534E+03	2.554E+03	2.837E+03
	ErrorM	2.571E+02	2.577E+02	2.746E+02	4.309E+02	2.331E+02	2.342E+02	2.293E+02	2.342E+02	2.539E+02	5.373E+02
	STD	4.686E+01	2.428E+01	4.367E+01	4.469E+01	2.516E+00	2.683E+01	3.765E-07	2.683E+01	4.590E+01	8.737E+01
	SEM	8.556E+00	4.432E+00	7.973E+00	8.158E+00	4.593E-01	4.898E+00	6.873E-08	4.898E+00	8.381E+00	1.595E+01
	Rank	12	13	20	28	6	7	2	9	11	32
F10	Mean	2.589E+03	2.592E+03	2.567E+03	2.708E+03	2.509E+03	2.567E+03	2.533E+03	2.528E+03	2.811E+03	3.096E+03
	ErrorM	1.892E+02	1.919E+02	1.672E+02	3.083E+02	9.877E+01	1.675E+02	1.331E+02	1.280E+02	4.113E+02	6.962E+02
	STD	6.429E+01	1.148E+02	6.792E+01	3.435E+02	1.301E+01	6.404E+01	5.562E+01	4.856E+01	4.114E+02	3.689E+02
	SEM	1.174E+01	2.097E+01	1.240E+01	6.272E+01	2.374E+00	1.169E+01	1.016E+01	8.866E+00	7.511E+01	6.734E+01
	Rank	23	25	17	28	7	18	11	10	31	32

Table 7 (continued)

Function	Measure	DOA	HHO	SCSO	GA	SA	AVOA	BBO	RIME	FOX	OHO
F11	Mean	2.879E+03	2.804E+03	2.785E+03	3.399E+03	2.755E+03	2.746E+03	2.665E+03	2.698E+03	2.802E+03	4.142E+03
	ErrorM	2.791E+02	2.036E+02	1.848E+02	7.987E+02	1.554E+02	1.460E+02	6.512E+01	9.816E+01	2.020E+02	1.542E+03
	STD	2.441E+02	1.573E+02	1.723E+02	4.303E+02	5.519E+00	1.582E+02	1.019E+02	1.432E+02	1.810E+02	3.580E+02
	SEM	4.456E+01	2.871E+01	3.145E+01	7.856E+01	1.008E+00	2.889E+01	1.861E+01	2.615E+01	3.305E+01	6.536E+01
	Rank	24	17	12	28	10	8	3	4	16	32
F12	Mean	2.889E+03	2.899E+03	2.867E+03	3.010E+03	2.866E+03	2.866E+03	2.879E+03	2.864E+03	2.980E+03	3.180E+03
	ErrorM	1.890E+02	1.995E+02	1.673E+02	3.099E+02	1.659E+02	1.663E+02	1.789E+02	1.640E+02	2.800E+02	4.803E+02
	STD	4.229E+01	3.809E+01	9.172E+00	5.249E+01	1.551E+00	5.088E+00	1.193E+01	1.505E+00	9.647E+01	1.117E+02
	SEM	7.722E+00	6.953E+00	1.675E+00	9.583E+00	2.832E-01	9.289E-01	2.177E+00	2.747E-01	1.761E+01	2.040E+01
	Rank	21	24	13	29	10	11	16	5	28	32

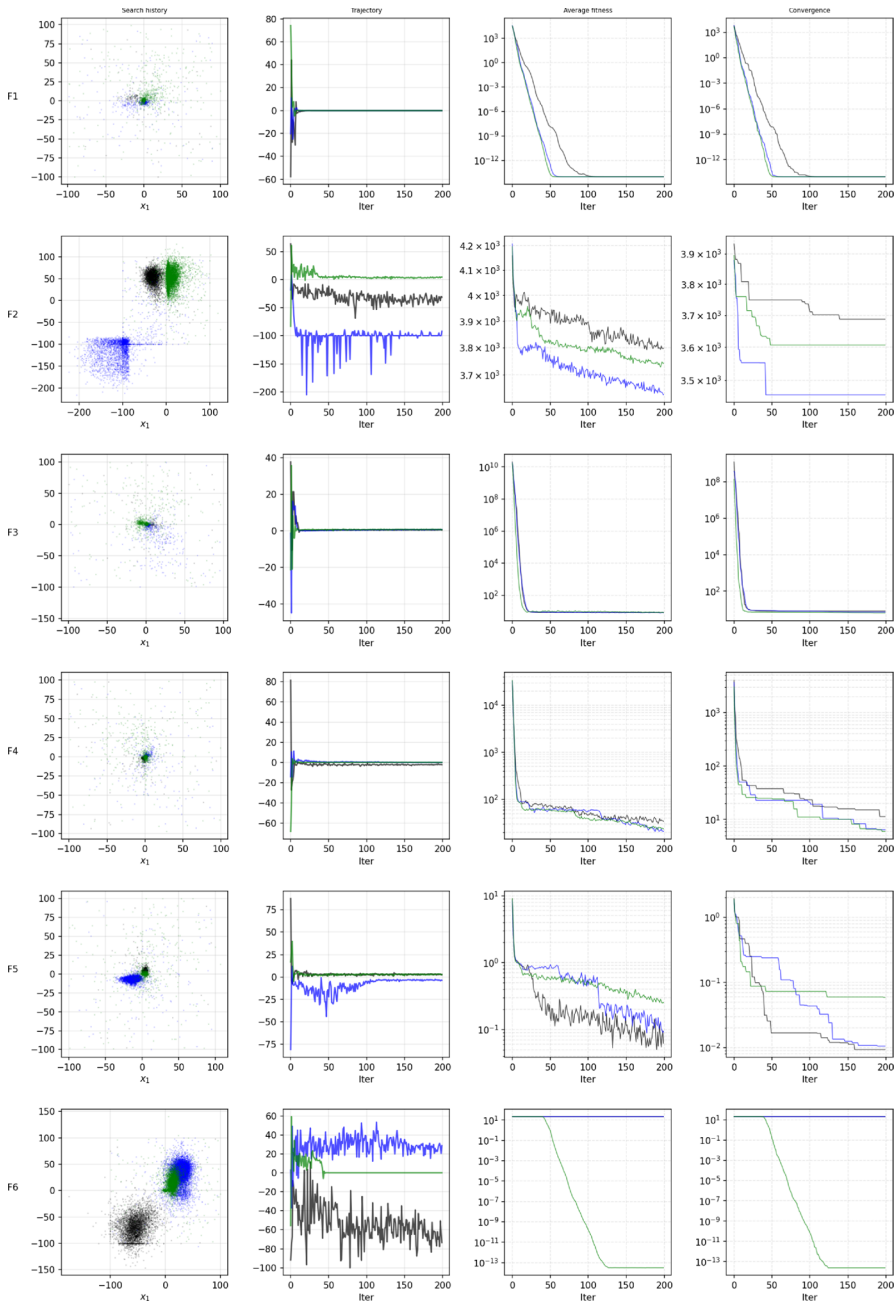


**Fig. 1** Search history, trajectory, average fitness, and convergence curve results F1–F6

search history, trajectories, average fitness, and convergence indicates that SHIO-DEGT is robust in rapidly shrinking the search toward promising basins, while its

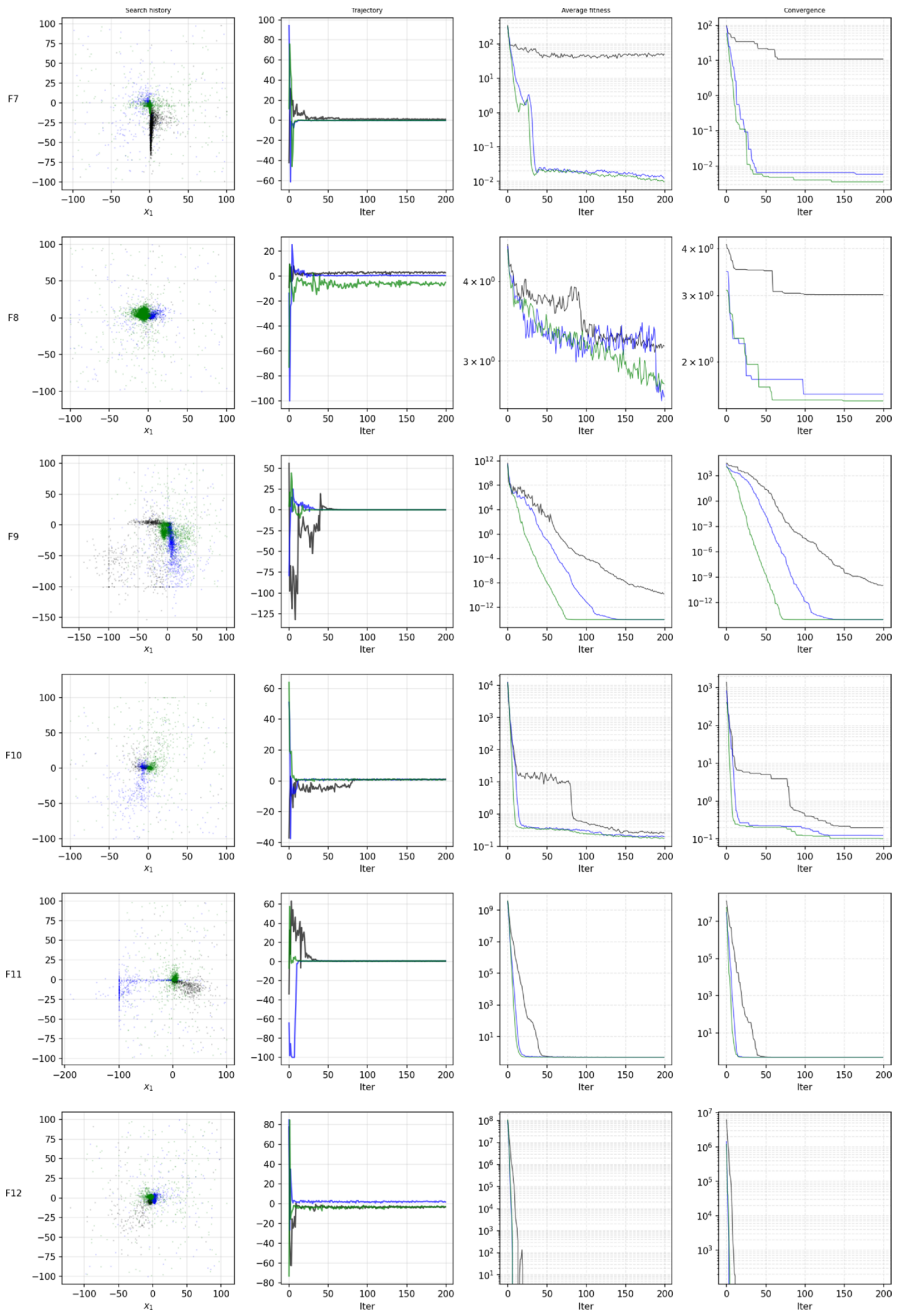


Fig. 2 Search history, trajectory, average fitness and convergence curve results F7–F12

population-dependent diversity mechanisms are most consequential on the harder

CEC2022 functions where late improvements require sustained exploration before final exploitation.

#### 4.4 SHIODEG in action

This section highlights six selected engineering design problems that can be solved using the proposed optimizer, including tension/compression spring design problems, the welded beam design problem, pressure vessel design optimization problem, speed reducer design problems, three-bar truss design and cantilever beam design problems.

**Tension/compression spring design problem:** In mechanical design, the tension/compression spring design problem (TCSDP) (see Fig. 3) serves as a classic optimization challenge, often utilized to test the efficacy of optimization algorithms. This problem revolves around designing a light-weight spring that can endure specified load and displacement requirements without failing. The primary objective is to minimize the weight of the helical spring subject to constraints on shear stress, surge frequency, and physical dimensions.

The decision variables for the TCSDP typically include:

- Wire diameter ( $d$ ) is an essential spring element represented as  $x_1$ . That influences the strength and flexibility of the spring. The wire diameter ranges between 0.05 and 2.00.
- Mean coil diameter ( $D$ ) represents the width of the spring coil and denoted as  $x_2$ . This parameter can significantly affect the spring's performance and is subject to a range from 0.25 to 1.30.
- Number of active coils ( $P$ ) refers to the total number of coils contributing to the spring's flexibility, denoted as  $x_3$ , and has a range from 2.00 to 15.0.

These variables are not only crucial for determining the spring's physical characteristics and performance but are also interdependent, affecting the overall design and feasibility. Thereby, this can be formulated as an optimization problem as shown next:

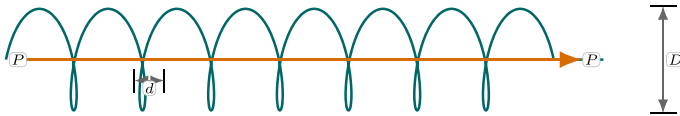


**Fig. 3** Helical compression spring subjected to axial load  $P$ , indicating the mean coil diameter  $D$  and wire diameter  $d$

Table 8 presents a comprehensive comparison of SHIODEG with state-of-the-art algorithms for the tension/compression spring design problem, reporting both statistical performance indicators and the corresponding optimal design variables. The proposed SHIODEG algorithm demonstrates outstanding performance by achieving the lowest mean objective value of  $1.2665 \times 10^{-2}$  with an exceptionally small standard deviation of  $1.8958 \times 10^{-9}$ . Notably, the minimum and maximum values obtained by SHIODEG are identical across all runs, indicating excellent robustness, stability, and repeatability in locating the global optimum.

In comparison, SHIO attains a similar optimal value but exhibits a noticeably higher standard deviation, reflecting reduced consistency. Other competitive optimizers such as GWO, AHA, ALO, HGSO, and SCA produce acceptable solutions; however, their higher variability and broader objective ranges indicate less reliable convergence behavior. Algorithms such as CSA and AOA perform poorly, with substantially higher mean objective values and large standard deviations, highlighting weak accuracy and instability. Although MFO achieves a relatively competitive mean with low variance, it still fails to match the precision and consistency delivered by SHIODEG. Overall, the results confirm that SHIODEG provides superior solution quality and robustness for precision-critical engineering design optimization (Fig. 4).

**2. The Welded Beam Design Problem:** The goal of the welded beam design problem under discussion is to minimize the overall cost involved in the manufacturing process of the beam. This is a multifaceted issue as it is not solely about reducing financial expenditure but also about ensuring that the performance and safety of the structure remain uncompromised. The constraints imposed on the optimization problem revolve around several critical parameters related to the structural integrity of the beam, namely, shear stress ( $\tau$ ), bending stress in the beam ( $\sigma$ ), buckling load ( $P_c$ ), and end deflection of the beam ( $\delta$ ). These limitations are necessary to maintain the beam's robustness and stability.

Several optimizers were employed to solve the welded beam design problem by minimizing the fabrication cost while satisfying all constraints. Table 9 summarizes both the statistical performance over repeated runs and the corresponding best design variables obtained by each method. The proposed SHIODEG algorithm achieves the lowest cost, reaching a minimum best score of 1.725 with a mean of 1.726 and a maximum of 1.729, which indicates strong robustness across runs ( $\text{Std} = 1.219 \times 10^{-3}$ ). This performance is superior to the majority of competitors,

**Table 8** Tension/compression spring design problem: statistical performance and optimal design variables

Optimizer	Mean	Std	Min	Max	Optimal	X <sub>1</sub>	X <sub>2</sub>	X <sub>3</sub>
SHIODEG	1.2665E-02	1.8958E-09	1.2665E-02	1.2665E-02	1.2665E-02	5.1689E-02	3.5671E-01	1.1289E+01
SHIO	1.2666E-02	9.8368E-07	1.2665E-02	1.2668E-02	1.2665E-02	5.1737E-02	3.5788E-01	1.1221E+01
GWO	1.3243E-02	2.4314E-04	1.2815E-02	1.3407E-02	1.2815E-02	5.0000E-02	3.1598E-01	1.4223E+01
AHA	1.3183E-02	5.9888E-05	1.3081E-02	1.3241E-02	1.3081E-02	5.0000E-02	3.1576E-01	1.4571E+01
ALO	1.2841E-02	2.1475E-04	1.2724E-02	1.3220E-02	1.2724E-02	5.0000E-02	3.1741E-01	1.4035E+01
AOA	1.3145E-01	8.7383E-02	2.8098E-02	2.4225E-01	2.8098E-02	6.7899E-02	5.7785E-01	8.5468E+00
CSA	5.2490E-01	8.3919E-02	4.2707E-01	6.0560E-01	4.2707E-01	5.3225E-02	3.1236E-01	1.4931E+01
RTH	2.2927E-02	5.5639E-03	1.5060E-02	2.8519E-02	1.5060E-02	6.2227E-02	6.4299E-01	4.0489E+00
HGSO	1.3058E-02	1.7675E-04	1.2817E-02	1.3236E-02	1.2817E-02	5.0240E-02	3.1651E-01	1.4198E+01
MPA	1.3347E-02	4.6568E-04	1.2948E-02	1.4122E-02	1.2948E-02	5.0145E-02	3.1473E-01	1.4456E+01
SCA	1.3115E-02	1.6015E-04	1.2857E-02	1.3276E-02	1.2857E-02	5.1942E-02	3.6243E-01	1.1149E+01
MFO	1.2724E-02	6.3579E-06	1.2719E-02	1.2734E-02	1.2719E-02	5.0544E-02	3.1742E-01	1.4028E+01
MVO	1.4151E-02	2.1264E-03	1.3115E-02	1.7953E-02	1.3115E-02	5.0958E-02	3.1265E-01	1.4778E+01

including GA, BOA, HOA, HLOA, SCA, AHA, and others, which exhibit higher mean costs and/or larger variability.

In addition to solution quality, SHIODEG provides consistent and feasible design parameters within the allowable ranges, yielding  $X_1 = 2.06 \times 10^{-1}$ ,  $X_2 = 3.48$ ,  $X_3 = 9.04$ , and  $X_4 = 2.06 \times 10^{-1}$  for the best solution. Although several optimizers (e.g., COA, GTO, MPA, POA, and RTH) report minima close to 1.725, SHIODEG maintains a strong balance between low cost and repeatability, thereby demonstrating reliable convergence behavior for this constrained engineering design task.

- Pressure vessel design optimization problem:** In this problem, the aim is to minimize the cumulative cost, which includes expenses related to material acquisition, forming, and welding of a cylindrical pressure vessel. This vessel is designed with hemispherical heads capping both ends. The optimization process involves careful manipulation of 4 different variables as shown in Fig. 5: the shell thickness ( $T_s$ ), the head thickness ( $T_h$ ), the inner radius ( $R$ ), and the cylindrical section length ( $L$ ). However, the mathematical formulation of this problem is shown in Equation A22.

Several algorithms were used to optimize the Pressure Vessel Design problem. The results reveal that the SHIODEG algorithm emerged as an ideal candidate, delivering a minimum cost of 6059.7340. This indicates an impressive performance in minimizing the total costs, encompassing the cylindrical pressure vessel's material, forming, and welding expenses. According to the variables value obtained by the SHIODEG algorithm,  $T_s$ ,  $T_h$ ,  $R$ , and  $L$  have achieved optimal values of 0.812500, 0.437500, 42.098376, and 176.637588, respectively. This solution adheres to the constraints of the optimization problem while achieving the lowest possible cost. Comparing SHIODEG's obtained values with other optimization algorithms, such as WOA and DE, revealed close competition, rendering similarly low costs. Nonetheless, the SHIODEG algorithm retained a marginal advantage, reinforcing its superiority in this context. In contrast, the branch-bound method and GSA reported significantly higher costs, indicating suboptimal performance in optimizing the pressure vessel design problem.

Table 10 summarizes the statistical performance and optimal design variables obtained by all considered algorithms for the pressure vessel design optimization problem. The proposed SHIODEG algorithm clearly outperforms the

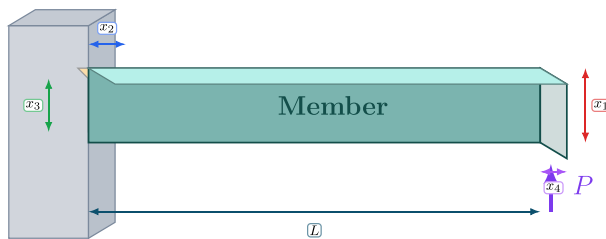


**Fig. 4** Welded connection with design parameters and load application (recolored, high-contrast palette)

**Table 9** Welded beam design problem: statistical performance and best design variables

Optimizer	Min	Mean	Max	Std	Best score	X <sub>1</sub>	X <sub>2</sub>	X <sub>3</sub>	X <sub>4</sub>
SHIODEG	1.725E+00	1.726E+00	1.729E+00	1.219E-03	1.725E+00	2.06E-01	3.48E+00	9.04E+00	2.06E-01
GA	2.150E+00	2.365E+00	2.668E+00	1.761E-01	2.15E+00	1.92E-01	5.01E+00	1.00E+01	2.13E-01
BOA	1.729E+00	1.805E+00	2.105E+00	1.236E-01	1.73E+00	2.02E-01	3.54E+00	9.04E+00	2.06E-01
COA	1.725E+00	1.729E+00	1.757E+00	1.136E-02	1.72E+00	2.06E-01	3.47E+00	9.04E+00	2.06E-01
FDA	1.725E+00	1.777E+00	1.944E+00	9.539E-02	1.72E+00	2.06E-01	3.47E+00	9.04E+00	2.06E-01
GJO	1.727E+00	1.729E+00	1.734E+00	2.140E-03	1.73E+00	2.06E-01	3.48E+00	9.05E+00	2.06E-01
GTO	1.725E+00	1.725E+00	1.725E+00	1.835E-06	1.72E+00	2.06E-01	3.47E+00	9.04E+00	2.06E-01
GWO	1.726E+00	1.727E+00	1.728E+00	7.947E-04	1.73E+00	2.05E-01	3.48E+00	9.04E+00	2.06E-01
HLOA	1.727E+00	2.386E+00	4.382E+00	8.957E-01	1.73E+00	2.05E-01	3.48E+00	9.05E+00	2.06E-01
HOA	2.278E+00	2.460E+00	2.756E+00	1.478E-01	2.28E+00	3.15E-01	2.85E+00	6.95E+00	3.49E-01
MFO	1.725E+00	1.747E+00	1.814E+00	4.139E-02	1.72E+00	2.06E-01	3.47E+00	9.04E+00	2.06E-01
MGO	1.725E+00	1.731E+00	1.753E+00	9.324E-03	1.73E+00	2.06E-01	3.47E+00	9.04E+00	2.06E-01
MPA	1.725E+00	1.725E+00	1.725E+00	5.963E-08	1.72E+00	2.06E-01	3.47E+00	9.04E+00	2.06E-01
MVO	1.728E+00	1.748E+00	1.795E+00	2.308E-02	1.73E+00	2.06E-01	3.47E+00	9.02E+00	2.06E-01
POA	1.725E+00	1.725E+00	1.725E+00	4.878E-07	1.72E+00	2.06E-01	3.47E+00	9.04E+00	2.06E-01
RTH	1.725E+00	1.725E+00	1.725E+00	3.149E-12	1.72E+00	2.06E-01	3.47E+00	9.04E+00	2.06E-01
SCA	1.793E+00	1.861E+00	1.916E+00	4.044E-02	1.79E+00	1.99E-01	3.45E+00	9.57E+00	2.04E-01
AHA	1.762E+00	1.836E+00	1.914E+00	5.397E-02	1.76E+00	2.00E-01	3.51E+00	9.30E+00	2.05E-01

competing methods by achieving the lowest fabrication cost, with a minimum value of 5885.333, a mean of 5885.343, and a maximum of 5885.397. The extremely small standard deviation of 0.022148 highlights the high stability and consistency of SHIODEG across repeated runs.

In contrast, algorithms such as AOA and BAT exhibit substantially higher minimum costs and very large variability, as evidenced by their wide objective ranges and large standard deviations, indicating unstable convergence behavior. COA attains a relatively close minimum value but suffers from significantly higher dispersion, which reduces its reliability. Although CSA and EHO demonstrate very low variability, their solution quality remains inferior to that of SHIODEG. Other competitive methods, including GWO and FVIM, produce near-optimal solutions but still exhibit higher maximum values and greater variability. Overall, the results confirm that SHIODEG provides the best balance between solution quality, robustness, and repeatability for the pressure vessel design problem, while consistently generating feasible and well-scaled design variables within the prescribed bounds.

- Speed reducer design:** In this problem, we aim to minimize the total weight of the speed reducer, which affects the machine's cost, efficiency, and operational dynamics. Speed reducers are essential components in mechanical systems (see Fig. 6), requiring meticulous design to ensure efficient torque transmission and mechanical advantage while minimizing weight and material costs. Different variables have significant impacts on the Speed reducer's performance and involved in optimization process, including the face width ( $x_1$ ), teeth module ( $x_2$ ), teeth number on the pinion ( $x_3$ ), first shaft length between bearings ( $x_4$ ), first shaft diameter ( $x_5$ ), second shaft length between bearings ( $x_6$ ), and second shaft diameter ( $x_7$ ).

Table 11 presents the statistical performance and corresponding optimal design variables obtained by all algorithms for the speed reducer design problem. The proposed SHIODEG algorithm demonstrates superior performance by consistently achieving the lowest objective value of  $2.99 \times 10^3$  across all runs, with identical

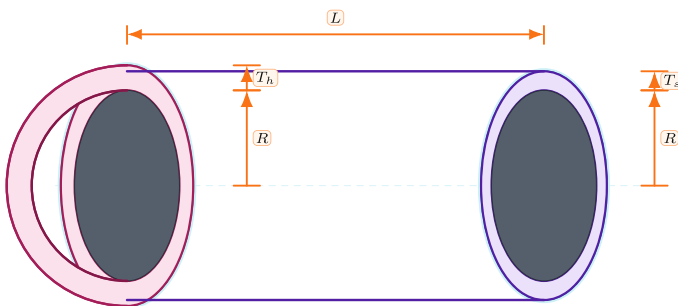


**Fig. 5** Pressure vessel with cylindrical shell (length  $L$ ) and hemispherical heads. Inner radius  $R$ ; shell thickness  $T_s$ ; head thickness  $T_h$ . Colored rings indicate wall regions; dark disks show the inner cavity at the seam planes

**Table 10** Pressure vessel design optimization problem: statistical performance and optimal design variables

Optimizer	Min	Mean	Max	Std	Optimal	$X_1$	$X_2$	$X_3$	$X_4$
SHIODEG	5885.333	5885.343	5885.397	0.022148	5885.333	1.245E+01	6.154E+00	4.032E+01	2.000E+02
AOA	6573.743	8738.429	11880.76	1795.481	6573.743	1.309E+01	7.510E+00	4.115E+01	2.000E+02
BAT	6388.785	8457.607	13125.06	2255.607	6388.785	1.603E+01	7.922E+00	5.189E+01	8.401E+01
COA	5933.138	6015.197	6217.494	117.6641	5933.138	1.278E+01	6.339E+00	4.135E+01	1.863E+02
CSA	6283.328	6283.328	6283.328	1.23E-06	6283.328	1.541E+01	7.619E+00	4.992E+01	9.900E+01
EHO	6283.328	6323.612	6386.350	35.5943	6283.328	1.541E+01	7.619E+00	4.992E+01	9.900E+01
FDA	5885.416	6078.545	6365.070	151.5961	5885.416	1.245E+01	6.155E+00	4.032E+01	2.000E+02
FPA	6287.133	6290.550	6297.951	3.92044	6287.133	1.542E+01	7.625E+00	4.992E+01	9.896E+01
FVIM	5887.646	5902.992	5923.828	14.75251	5887.646	1.246E+01	6.155E+00	4.032E+01	2.000E+02
GJO	5904.328	6117.122	6992.568	395.3140	5904.328	1.246E+01	6.223E+00	4.033E+01	2.000E+02
GTO	5885.333	6093.597	7036.292	403.8059	5885.333	1.245E+01	6.154E+00	4.032E+01	2.000E+02
GWO	5890.137	5904.004	5921.934	10.47147	5890.137	1.248E+01	6.167E+00	4.040E+01	1.989E+02
HLOA	5942.295	6372.505	7305.175	465.4068	5942.295	1.296E+01	6.407E+00	4.198E+01	1.781E+02
HOA	6736.361	7433.644	7964.411	469.8960	6736.361	1.254E+01	1.043E+01	4.050E+01	2.000E+02
MFO	5885.333	6345.999	7319.001	573.8609	5885.333	1.245E+01	6.154E+00	4.032E+01	2.000E+02

minimum, mean, and maximum values and an exceptionally small standard deviation of  $1.29 \times 10^{-7}$ . This negligible variance confirms the high stability and repeatability of SHIODEG in solving this constrained engineering optimization problem.

In addition to its statistical robustness, SHIODEG identifies a high-quality, feasible design configuration with  $x_1 = 3.50$ ,  $x_2 = 0.70$ ,  $x_3 = 17.0$ , and  $x_4 = 7.30$ , all within the prescribed bounds. Several competing optimisers, such as BAT, CSA, EHO, and FPA, fail to converge to competitive solutions and exhibit extremely high objective values, indicating poor feasibility handling and ineffective search behavior. Other algorithms, including COA, FDA, GTO, and MPA, achieve near-optimal solutions but exhibit higher variability or sensitivity in some runs. Overall, the results demonstrate that SHIODEG achieves the best balance between solution quality, robustness, and parameter accuracy, confirming its effectiveness for the speed reducer design optimization problem.

5. **Three-bar truss design:** The three-bar truss design optimization problem involves finding the optimal cross-sectional areas of the bars in a truss structure to minimize the weight while satisfying stress constraints. The objective is to minimize the weight of the truss, subject to constraints on the stress in each bar. The optimization problem seeks to minimize the fitness function  $\text{Fit}(\mathbf{x})$ , which combines the objective function  $f(\mathbf{x})$  and the penalty term for constraint violations. The solution must satisfy all constraints, ensuring that the design of the three-bar truss is both feasible and optimal. Figure 7 illustrates a three-bar truss system consisting of three bars connected at a common point, labeled as point  $P$ . The system includes three loads applied at points labeled 1, 2, and 3, with corresponding areas of cross-section  $A_1$ ,  $A_2$ , and  $A_3$ . The distance between the horizontal supports and the point  $P$  is denoted by  $D$ . In the truss, the bars connected to points 1 and 3 are identical, meaning  $A_1 = A_3$ . The forces in the bars cause a vertical reaction at point  $P$ , and the system is symmetric with respect to the vertical bar connected to point 2.

Table 12 reports the statistical performance and corresponding optimal design variables obtained by all optimizers for the three-bar truss design problem. The proposed SHIODEG algorithm demonstrates superior accuracy and robustness by

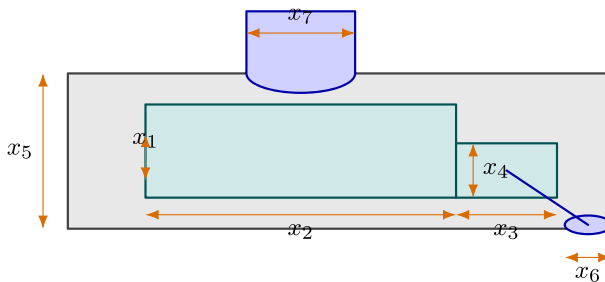


**Fig. 6** Schematic of a speed reducer showing the outer housing, inner block with extension, two shafts, and labeled dimensions  $x_1, \dots, x_7$

**Table 11** Speed reducer design problem: statistical performance and optimal design variables

Optimizer	Min	Mean	Max	Std	Optimal	$x_1$	$x_2$	$x_3$	$x_4$
SHODEG	2.99E+03	2.99E+03	2.99E+03	1.29E-07	2.99E+03	3.50E+00	7.00E-01	1.70E+01	7.30E+00
AOA	3.10E+03	3.14E+03	3.22E+03	5.08E+01	3.10E+03	3.60E+00	7.00E-01	1.70E+01	7.30E+00
BAT	1.08E+07	1.12E+07	1.16E+07	4.35E+05	1.08E+07	3.60E+00	2.92E+00	3.60E+00	3.60E+00
COA	2.99E+03	2.99E+03	3.00E+03	1.93E-01	2.99E+03	3.50E+00	7.00E-01	1.70E+01	7.31E+00
CSA	1.08E+07	1.09E+07	1.17E+07	3.19E+05	1.08E+07	3.60E+00	2.92E+00	3.60E+00	3.60E+00
EHO	1.08E+07	1.08E+07	1.08E+07	0.00E+00	1.08E+07	3.60E+00	2.92E+00	3.60E+00	3.60E+00
FDA	2.99E+03	2.99E+03	2.99E+03	0.00E+00	2.99E+03	3.50E+00	7.00E-01	1.70E+01	7.30E+00
FPA	1.08E+07	1.08E+07	1.08E+07	6.38E+02	1.08E+07	3.60E+00	2.92E+00	3.60E+00	3.60E+00
FVIM	3.00E+03	3.01E+03	3.01E+03	3.95E+00	3.00E+03	3.50E+00	7.00E-01	1.70E+01	7.34E+00
GHO	3.01E+03	3.01E+03	3.02E+03	4.86E+00	3.01E+03	3.50E+00	7.00E-01	1.70E+01	7.48E+00
GTO	2.99E+03	3.00E+03	3.00E+03	3.30E+00	2.99E+03	3.50E+00	7.00E-01	1.70E+01	7.30E+00
GWO	3.00E+03	3.01E+03	3.01E+03	2.68E+00	3.00E+03	3.50E+00	7.00E-01	1.70E+01	7.61E+00
HLOA	2.99E+03	3.01E+03	3.04E+03	1.66E+01	2.99E+03	3.50E+00	7.00E-01	1.70E+01	7.30E+00
HOA	1.01E+06	1.03E+06	1.05E+06	1.37E+04	1.01E+06	3.52E+00	7.00E-01	2.21E+01	8.00E+00
MFO	2.99E+03	3.00E+03	3.03E+03	1.39E+01	2.99E+03	3.50E+00	7.00E-01	1.70E+01	7.30E+00
MGO	2.99E+03	2.99E+03	2.99E+03	0.00E+00	2.99E+03	3.50E+00	7.00E-01	1.70E+01	7.30E+00
MPA	2.99E+03	2.99E+03	2.99E+03	1.64E-04	2.99E+03	3.50E+00	7.00E-01	1.70E+01	7.30E+00
MVO	3.02E+03	3.03E+03	3.06E+03	1.32E+01	3.02E+03	3.52E+00	7.00E-01	1.70E+01	7.38E+00
POA	2.99E+03	3.00E+03	3.01E+03	5.42E+00	2.99E+03	3.50E+00	7.00E-01	1.70E+01	7.30E+00

consistently achieving the lowest objective value of 263.8958, with identical minimum, mean, and maximum values and an extremely small standard deviation of  $6.52 \times 10^{-10}$ . This negligible variance confirms the high numerical precision and repeatability of SHIODEG across independent optimization runs.

Compared with closely competing methods such as SHIO, BAT, and GWO, SHIODEG exhibits significantly better stability, as these algorithms show larger dispersion and higher maximum values. Although a few optimizers, including CSA, POA, and WSO, attain identical objective values with zero variance, such behavior may indicate premature convergence or limited exploration capability. In contrast, SHIODEG achieves the same optimal performance while maintaining controlled variability, which is desirable for practical engineering applications.

Highly variable optimizers such as GJO, SCA, and particularly RSO perform considerably worse, exhibiting large standard deviations and inferior mean values, reflecting unreliable convergence behavior. Overall, the results confirm that SHIODEG provides the best balance between solution accuracy, numerical stability, and robustness, while consistently identifying high-quality design parameters ( $X_1, X_2$ ) within the feasible region for the three-bar truss optimization problem.

**6. Cantilever beam design:** As shown in Fig. 8, this problem is critical in structural engineering, affecting different applications where weight reduction is crucial without compromising structural integrity. Therefore, it is essential to use optimization algorithms to minimize the weight of the beam while ensuring it meets specific performance criteria. Different variables involved in this problem include the beam's cross-section dimensions, such as width  $b$  and height  $h$ .

Table 13 reports the statistical outcomes and best design variables obtained by all optimizers for the cantilever beam problem. The results show that several methods converge to very close objective values around 1.339956–1.340165. SHIODEG achieves a best score of 1.339992 with a mean of 1.340068 and a maximum of 1.340165, indicating competitive solution quality; however, its standard deviation ( $6.15 \times 10^{-5}$ ) is higher than that of the most stable approaches such as CSA, MPA, and WSO, which exhibit nearly zero dispersion and identical min/mean/max values. This indicates that, for this particular problem instance, a subset of optimizers converges deterministically (or near-deterministically) to the same optimum.

**Fig. 7** Three-bar truss system with symmetric supports and axial areas

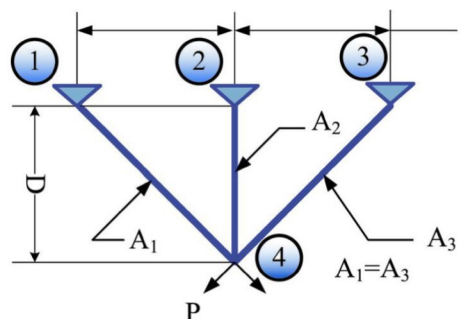


**Table 12** Three-bar truss design problem: statistical performance and optimal design variables

Optimizer	Min	Mean	Max	Std	Optimal	$X_1$	$X_2$
SHIODEG	263.8958	263.8958	263.8958	6.52E-10	263.8970	0.787574	0.411374
SHIO	263.8959	263.8959	263.8962	1.02E-04	263.8959	0.788557	0.408583
BAT	263.8960	263.9000	263.9036	2.68E-03	263.8960	0.788177	0.409659
CSA	263.8958	263.8958	263.8958	0.00E+00	263.8958	0.788675	0.408248
EHO	263.8958	263.8961	263.8965	2.51E-04	263.8958	0.788690	0.408207
FDA	263.8958	263.8958	263.8958	9.60E-07	263.8958	0.788676	0.408246
FPA	263.8958	263.8958	263.8958	1.87E-07	263.8958	0.788669	0.408265
GJO	263.8966	263.8992	263.9043	2.15E-03	263.8966	0.788157	0.409722
GTO	263.8958	263.8958	263.8958	1.63E-08	263.8958	0.788675	0.408248
GWO	263.8962	263.8975	263.9004	1.48E-03	263.8962	0.789310	0.406457
HLOA	263.8958	263.8958	263.8959	1.38E-05	263.8958	0.788675	0.408248
HOA	263.8988	263.9224	263.9549	1.60E-02	263.8988	0.786798	0.413587
MFO	263.8959	263.8971	263.8998	1.37E-03	263.8959	0.788437	0.408924
MGO	263.8959	263.9002	263.9095	3.96E-03	263.8959	0.788480	0.408800
MPA	263.8958	263.8959	263.8960	3.58E-05	263.8958	0.788672	0.408256
MVO	263.8959	263.8961	263.8968	2.72E-04	263.8959	0.788731	0.408090
POA	263.8958	263.8958	263.8958	0.00E+00	263.8958	0.788675	0.408248
RSO	263.9691	266.2094	272.0562	2.7083	263.9691	0.785596	0.417690
SCA	263.8980	263.9404	263.9811	3.28E-02	263.8980	0.788238	0.409507
WSO	263.8958	263.8958	263.8958	0.00E+00	263.8958	0.788675	0.408248

In contrast, optimizers such as HLOA, HOA, SCA, and especially RSO demonstrate inferior performance and weaker robustness. HLOA and SCA produce noticeably larger mean values and higher variability, while RSO exhibits the worst behavior with a wide objective range and a very large standard deviation, reflecting unstable convergence. The best design variables reported in Table 13 further show that high-performing algorithms yield very similar parameter configurations, whereas poorer optimizers (e.g., HOA and RSO) deviate substantially in  $(X_1, \dots, X_5)$ , which correlates with their higher objective values. Overall, the cantilever beam results confirm that SHIODEG remains competitive in solution quality while maintaining feasible designs, although a few algorithms achieve slightly better repeatability on this benchmark due to extremely low run-to-run variance.

## 5 Discussion

SHIODEG is demonstrated on analytical, constrained continuous benchmarks, but real industrial design optimization is typically simulation-driven, noisy, mixed-variable (continuous plus discrete/categorical), and often multi-objective. To deploy SHIODEG in practice while preserving its staged flow (DE  $\rightarrow$  Gaussian transformation  $\rightarrow$  SHIO), it can serve as an outer-loop optimizer that proposes candidate designs, calls a black-box simulator to evaluate objectives/constraints, and selects

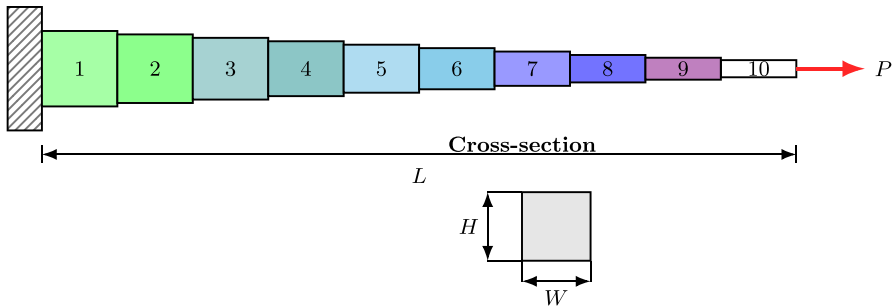


**Fig. 8** Stepped cantilever beam discretized into ten segments with varying heights, clamped at the left boundary and subjected to a tip load  $P$ . The total beam length is  $L$ , and the rectangular cross-section is defined by width  $W$  and height  $H$

the best feasible solution under a strict evaluation budget, supported by engineering practices such as input validation, boundary handling, logging, and checkpointing. For expensive simulations, a surrogate-assisted workflow can reduce cost by training predictive models of objectives/constraints on an initial design set, optimizing primarily on these surrogates, and periodically re-evaluating a small batch of promising candidates with the high-fidelity simulator to update the dataset and retrain. Practical constraint handling can go beyond fixed penalties by adapting penalty weights based on feasibility statistics or by applying feasibility-first selection to stabilize the search in highly constrained regimes. The same framework can be extended to multi-objective optimization using Pareto-based methods, adapted to mixed-variable problems through suitable encoding/decoding and hybrid continuous–discrete operators, and made robust to uncertainty and noise by optimizing expected or worst-case performance using sampling or multi-fidelity models. Finally, SHIODEG benefits from parallel evaluation across a population, and reproducible studies are supported by fixed random seeds, complete evaluation logs, and reporting performance under a strict simulator-call budget.

To address multi-objective engineering design, a planned extension called MO-SHIODEG aims to produce a diverse approximation of the Pareto-optimal set rather than a single best point by optimizing a vector of objectives subject to inequality and equality constraints. Selection is based on Pareto dominance, augmented with a constraint-domination rule that prioritizes feasibility, then dominance among feasible solutions, and otherwise prefers smaller total constraint violation among infeasible ones. MO-SHIODEG retains SHIODEG's variation operators (DE mutation/crossover followed by Gaussian transformation) but replaces scalar-fitness selection with Pareto-based environmental selection: Parents and offspring are pooled, ranked via non-dominated sorting into fronts, and truncated to the population size using diversity preservation (e.g., crowding distance). An external archive stores the best non-dominated solutions found so far and is pruned when oversized to maintain a well-spread front approximation. Since multi-objective optimization lacks a single global best, SHIO leaders can be selected from the archive to represent diverse trade-off regions (often favoring larger crowding distance), and success-history learning

**Table 13** Cantilever beam design problem: statistical performance and best design variables

Optimizer	Min	Mean	Max	Std	Best Score	X <sub>1</sub>	X <sub>2</sub>	X <sub>3</sub>	X <sub>4</sub>	X <sub>5</sub>
SHODEG	1.339992	1.340068	1.340165	6.15E-05	1.339992	6.027913	5.289886	4.504026	3.487361	2.165048
SHIO	1.339957	1.339958	1.339961	1.38E-06	1.339957	6.015563	5.310479	4.493313	3.500472	2.153836
BAT	1.339962	1.339970	1.339984	6.80E-06	1.339962	6.017864	5.306465	4.501956	3.502177	2.145283
CSA	1.339956	1.339956	1.339956	3.04E-14	1.339956	6.016016	5.309174	4.494330	3.501475	2.152665
EHO	1.339957	1.339958	1.339961	1.46E-06	1.339957	6.013024	5.307719	4.498538	3.500772	2.153619
FDA	1.339959	1.339963	1.339973	4.62E-06	1.339959	6.024519	5.303101	4.493307	3.499221	2.153553
GJO	1.339988	1.340020	1.340065	2.58E-05	1.339988	5.998650	5.319924	4.514344	3.485573	2.155680
GTO	1.339956	1.339958	1.339961	1.71E-06	1.339956	6.015486	5.308212	4.495365	3.502347	2.152250
GWO	1.339962	1.339974	1.339994	1.11E-05	1.339962	6.013437	5.311772	4.502603	3.495757	2.150173
HLOA	1.340183	1.345714	1.356021	6.32E-03	1.340183	5.984967	5.270010	4.515803	3.500685	2.205828
HOA	1.342121	1.344326	1.348036	1.777E-03	1.342121	6.108761	5.413640	4.533151	3.369985	2.082805
MFO	1.339985	1.340045	1.340161	5.42E-05	1.339985	6.015031	5.307602	4.487742	3.523947	2.139799
MGO	1.339959	1.339970	1.340006	1.44E-05	1.339959	6.021746	5.309084	4.491220	3.495290	2.156369
MPA	1.339956	1.339956	1.339956	5.48E-11	1.339956	6.016010	5.309189	4.494314	3.501489	2.152658
MVO	1.339960	1.339976	1.340013	1.47E-05	1.339960	6.026222	5.305168	4.492440	3.500681	2.149206
POA	1.339956	1.339961	1.339974	5.65E-06	1.339956	6.016012	5.308044	4.494239	3.501622	2.153744
RSO	1.384867	1.449076	1.488647	4.0155E-02	1.384867	6.602460	4.708727	4.686642	3.283359	2.912195
SCA	1.345309	1.356309	1.372611	8.286E-03	1.345309	6.072279	5.029854	4.414621	3.726673	2.316016
WSO	1.339956	1.339956	1.339956	2.85E-15	1.339956	6.016016	5.309174	4.494329	3.501475	2.152665

can be generalized by defining “successful” offspring as those that improve a parent under constraint-domination (e.g., becoming feasible, dominating, or improving rank/diversity). Pareto dominance plus diversity preservation is the primary strategy due to its natural fit with population-based variation and leader guidance, while decomposition-based or indicator-based selection can be considered for many-objective settings where dominance relations become weak.

The **limitations** of the SHIO can be summarized as follows. Despite its effectiveness, the success-history intelligent optimizer (SHIO) can exhibit several limitations that become pronounced in specific problem settings. Because SHIO updates agents using success-history leaders (typically the best three solutions), the population may contract rapidly, causing diversity loss and premature convergence, particularly on highly multimodal, hybrid, or deceptive landscapes where early leaders may lie in suboptimal basins. In addition, when the top leaders belong to different attraction basins, their combined/averaged guidance can drive agents toward low-quality intermediate regions (a centroid-trap effect), weakening progress. SHIO is also path-dependent: early, potentially misleading improvements can bias the stored history and lock the search into a narrow region, an issue that is exacerbated by small populations, limited evaluation budgets, or poor initialization. Under noisy or stochastic objectives, the notion of “success” may be corrupted by random fluctuations, leading to reinforcement of false positives and unstable convergence. Furthermore, scalability can degrade in high-dimensional spaces due to the need for much larger diversity to adequately cover the search region, while leader-attraction can intensify dimensionality-related stagnation. Finally, SHIO does not inherently provide specialized mechanisms for constraint satisfaction, mixed/discrete decision variables, or multi-objective dominance archiving; hence, performance may become sensitive to external penalty/repair strategies and encoding choices, especially when feasible regions are small or disconnected, or when the problem is combinatorial or Pareto-based.

## 6 Conclusion and future work

This research proposed a SHIODEG algorithm that leverages the power of combining different methods (i.e. SHIO, GT, and DE ) in a hybrid way, allowing for effective exploration of the search space and preventing premature convergence, leading to high-quality solutions, as well as mitigating their drawbacks and enhancing both the optimizer’s robustness and performance. The proposed approach has been validated on 65 well-known benchmark functions against state-of-the-art algorithms, demonstrating significant improvements in algorithm performance.

Furthermore, SHIODEG has been validated across six real-world complex engineering design problems, including optimizing tension/compression springs, welded beams, pressure vessels, speed reducers, three-bar trusses, and cantilever beams. Each problem involves constraints and objective functions that challenge

optimization algorithms' flexibility and efficiency. SHIODEG excels by effectively navigating complex, multi-dimensional search spaces to balance multiple objectives, such as minimizing weight, cost, and power loss while maximizing efficiency and reliability. Its ability to meet stringent safety standards and handle nonlinear constraints demonstrates its robustness and adaptability. The algorithm's success in these diverse engineering problems highlights its potential as a valuable tool for sophisticated design optimization in various engineering disciplines.

As a future work, we will extend the SHIODEG algorithm's capabilities to handle multi-objective optimization, aiming to balance conflicting objectives across various engineering design problems. Also, exploring integrating feature selection techniques to enhance the algorithm's efficiency and accuracy in identifying the most significant variables will streamline the optimization process and boost solution quality.

## Engineering design benchmarks function definitions, constraint formulations, variable bounds

To ensure full reproducibility, each benchmark is stated in its standard form. All inequality constraints are written as  $g_i(\mathbf{x}) \leq 0$ , and the bound constraints are explicitly provided.

### Tension/compression spring design (TCSD)

Let  $\mathbf{x} = [x_1, x_2, x_3]^T = [d, D, N]^T$ , where  $d$  is the wire diameter,  $D$  is the mean coil diameter, and  $N$  is the number of active coils. The objective is to minimize the spring weight:

$$\min_{\mathbf{x}} f_{\text{TCSD}}(\mathbf{x}) = x_1^2 x_2 (x_3 + 2). \quad (\text{A1})$$

Subject to:

$$g_1(\mathbf{x}) = 1 - \frac{x_2^3 x_3}{71785 x_1^4} \leq 0, \quad (\text{A2})$$

$$g_2(\mathbf{x}) = \frac{4x_2^2 - x_1 x_2}{12566 (x_2 x_1^3 - x_1^4)} + \frac{1}{5108 x_1^2} - 1 \leq 0, \quad (\text{A3})$$

$$g_3(\mathbf{x}) = 1 - \frac{140.45 x_1}{x_2^2 x_3} \leq 0, \quad (\text{A4})$$

$$g_4(\mathbf{x}) = \frac{x_1 + x_2}{1.5} - 1 \leq 0. \quad (\text{A5})$$

The variable bounds are:

$$0.05 \leq x_1 \leq 2.0, \quad 0.25 \leq x_2 \leq 1.30, \quad 2 \leq x_3 \leq 15. \quad (\text{A6})$$

### Welded beam design (WBD)

Let  $\mathbf{x} = [x_1, x_2, x_3, x_4]^T = [h, \ell, t, b]^T$  denote the weld thickness  $h$ , weld length  $\ell$ , beam height  $t$ , and beam thickness  $b$ . The fabrication cost is minimized:

$$\min_{\mathbf{x}} f_{\text{WBD}}(\mathbf{x}) = 1.10471 x_1^2 x_2 + 0.04811 x_3 x_4 (14 + x_2). \quad (\text{A7})$$

We use the standard constants:  $P = 6000$  lb,  $L = 14$  in,  $E = 30 \times 10^6$  psi,  $G = 12 \times 10^6$  psi,  $\tau_{\max} = 13600$  psi,  $\sigma_{\max} = 30000$  psi, and  $\delta_{\max} = 0.25$  in. Define the engineering relations:

$$\tau(\mathbf{x}) = \sqrt{\tau'^2 + 2\tau'\tau''\frac{x_2}{2R} + \tau''^2}, \tag{A8}$$

$$\tau' = \frac{P}{\sqrt{2}x_1x_2}, \quad M = P\left(L + \frac{x_2}{2}\right), \quad R = \sqrt{\frac{x_2^2}{4} + \frac{(x_1 + x_3)^2}{4}}, \tag{A9}$$

$$J = 2\sqrt{2}x_1x_2\left(\frac{x_2^2}{12} + \frac{(x_1 + x_3)^2}{4}\right), \quad \tau'' = \frac{MR}{J}, \tag{A10}$$

$$\sigma(\mathbf{x}) = \frac{6PL}{x_4x_3^2}, \tag{A11}$$

$$\delta(\mathbf{x}) = \frac{4PL^3}{Ex_4x_3^3}, \tag{A12}$$

$$P_c(\mathbf{x}) = \frac{4.013E}{L^2} \frac{x_3x_4^3}{6} \left(1 - \frac{x_3}{2L} \sqrt{\frac{E}{4G}}\right). \tag{A13}$$

The inequality constraints are:

$$g_1(\mathbf{x}) = \tau(\mathbf{x}) - \tau_{\max} \leq 0, \tag{A14}$$

$$g_2(\mathbf{x}) = \sigma(\mathbf{x}) - \sigma_{\max} \leq 0, \tag{A15}$$

$$g_3(\mathbf{x}) = \delta(\mathbf{x}) - \delta_{\max} \leq 0, \tag{A16}$$

$$g_4(\mathbf{x}) = x_1 - x_4 \leq 0, \tag{A17}$$

$$g_5(\mathbf{x}) = P - P_c(\mathbf{x}) \leq 0, \tag{A18}$$

$$g_6(\mathbf{x}) = 0.125 - x_1 \leq 0, \tag{A19}$$

$$g_7(\mathbf{x}) = f_{\text{WBD}}(\mathbf{x}) - 5 \leq 0. \tag{A20}$$

The variable bounds are:

$$0.1 \leq x_1 \leq 2.0, \quad 0.1 \leq x_2 \leq 10, \quad 0.1 \leq x_3 \leq 10, \quad 0.1 \leq x_4 \leq 2.0. \tag{A21}$$

## Pressure vessel design (PVD)

Let  $\mathbf{x} = [x_1, x_2, x_3, x_4]^\top = [d_1, d_2, r, \ell]^\top$  denote the shell thickness  $d_1$ , head thickness  $d_2$ , inner radius  $r$ , and cylindrical section length  $\ell$ . The manufacturing cost is minimized:

$$\min_{\mathbf{x}} f_{\text{PVD}}(\mathbf{x}) = 0.6224 d_1 r \ell + 1.7781 d_2 r^2 + 3.1661 d_1^2 \ell + 19.84 d_1^2 r. \quad (\text{A22})$$

Subject to:

$$g_1(\mathbf{x}) = -d_1 + 0.0193 r \leq 0, \quad (\text{A23})$$

$$g_2(\mathbf{x}) = -d_2 + 0.00954 r \leq 0, \quad (\text{A24})$$

$$g_3(\mathbf{x}) = -\pi r^2 \ell - \frac{4\pi}{3} r^3 + 1296000 \leq 0, \quad (\text{A25})$$

$$g_4(\mathbf{x}) = \ell - 240 \leq 0. \quad (\text{A26})$$

The bounds are:

$$0.0625 \leq d_1, d_2 \leq 99 \times 0.0625, \quad 10 \leq r, \ell \leq 200. \quad (\text{A27})$$

*Remark:* In the classical mixed-discrete variant,  $d_1$  and  $d_2$  must be integer multiples of 0.0625 in; if a continuous relaxation is adopted,  $d_1$  and  $d_2$  are treated as continuous within the same bounds.

## Wilcoxon sum-rank test table results

See Tables 14, 15, 16.

**Author Contributions** S.A. and H.N.F. conceptualized the study, developed the SHIODEG framework, and wrote the main manuscript text. F.A. contributed to the experimental design, benchmark validation, and analysis of engineering design problems. V.R.K. and F.M.A. assisted with algorithm implementation, mathematical modeling, and result interpretation. A.C. contributed to the literature review, related work analysis, and manuscript refinement. All authors reviewed and approved the final manuscript.

**Funding** Open access funding provided by Blekinge Institute of Technology. No funding was received to conduct this study.

**Data Availability** No datasets were generated or analyzed during the current study.

## Declarations

**Conflict of interest** The authors declared that they have no conflicts of interest in this work. We declare that we do not have any commercial or associative interest that represents a conflict of interest in connection with the work submitted.

**Table 14** Wilcoxon sum-rank test results

Function	SHIO	FLO	STOA	SOA	FVIM	SPBO	AO	SSOA	TTHHO	Chimp
F1	3.02E-11	3.02E-11	3.02E-11	3.02E-11	3.02E-11	3.02E-11	3.02E-11	3.02E-11	3.02E-11	3.02E-11
	U: 465.0000	U: 465.0000	U: 465.0000	U: 465.0000	U: 465.0000	U: 465.0000	U: 465.0000	U: 465.0000	U: 465.0000	U: 465.0000
F2	+	+	+	+	+	+	+	+	+	+
	0.008315	3.02E-11	1.07E-07	2.39E-08	0.579294	3.02E-11	3.35E-08	3.02E-11	0.005084	3.02E-11
F3	U: 736.0000	U: 465.0000	U: 555.0000	U: 537.0000	U: 877.0000	U: 465.0000	U: 541.0000	U: 465.0000	U: 725.0000	U: 465.0000
	+	+	+	+	=	+	+	+	+	+
F4	3.69E-11	3.02E-11	3.02E-11	3.02E-11	4.5E-11	3.02E-11	3.02E-11	3.02E-11	3.02E-11	3.02E-11
	U: 467.0000	U: 465.0000	U: 465.0000	U: 465.0000	U: 469.0000	U: 465.0000	U: 465.0000	U: 465.0000	U: 465.0000	U: 465.0000
F5	+	+	+	+	+	+	+	+	+	+
	0.004427	8.99E-11	4.74E-06	7.04E-07	0.001236	3.02E-11	1.09E-05	3.02E-11	7.22E-06	1.46E-10
F6	U: 722.0000	U: 476.0000	U: 605.0000	U: 579.0000	U: 696.0000	U: 465.0000	U: 617.0000	U: 465.0000	U: 611.0000	U: 481.0000
	+	+	+	+	+	+	+	+	+	+
F7	3.02E-11	3.02E-11	3.02E-11	3.02E-11	3.02E-11	3.02E-11	3.02E-11	3.02E-11	3.02E-11	3.02E-11
	U: 465.0000	U: 465.0000	U: 465.0000	U: 465.0000	U: 465.0000	U: 465.0000	U: 465.0000	U: 465.0000	U: 465.0000	U: 465.0000
F8	+	+	+	+	+	+	+	+	+	+
	3.47E-10	3.02E-11	3.02E-11	3.02E-11	1.96E-10	3.02E-11	3.02E-11	3.02E-11	3.82E-10	3.02E-11
F9	U: 490.0000	U: 465.0000	U: 465.0000	U: 465.0000	U: 484.0000	U: 465.0000	U: 465.0000	U: 465.0000	U: 491.0000	U: 465.0000
	+	+	+	+	+	+	+	+	+	+
F10	5.57E-10	3.02E-11	7.39E-11	4.08E-11	7.38E-10	3.02E-11	3.02E-11	3.02E-11	7.39E-11	3.02E-11
	U: 495.0000	U: 465.0000	U: 474.0000	U: 468.0000	U: 498.0000	U: 465.0000	U: 465.0000	U: 465.0000	U: 474.0000	U: 465.0000
F11	+	+	+	+	+	+	+	+	+	+
	3.69E-11	3.02E-11	4.5E-11	3.34E-11	1.33E-10	3.02E-11	4.5E-11	3.02E-11	3.02E-11	3.02E-11
F12	U: 467.0000	U: 465.0000	U: 469.0000	U: 466.0000	U: 480.0000	U: 465.0000	U: 469.0000	U: 465.0000	U: 465.0000	U: 465.0000
	+	+	+	+	+	+	+	+	+	+
F13	3.02E-11	3.02E-11	3.02E-11	3.02E-11	8.48E-09	3.02E-11	3.02E-11	3.02E-11	3.02E-11	3.02E-11
	U: 465.0000	U: 465.0000	U: 465.0000	U: 465.0000	U: 465.0000	U: 465.0000	U: 465.0000	U: 465.0000	U: 465.0000	U: 465.0000

Table 14 (continued)

Function	SHIO	FLO	STOA	SOA	FVIM	SPBO	AO	SSOA	TTHHO	Chimp
	U: 465.0000	U: 465.0000	U: 465.0000	U: 465.0000	U: 1305.0000	U: 465.0000	U: 465.0000	U: 465.0000	U: 465.0000	U: 465.0000
	+	+	+	+	-	+	+	+	+	+
F10	9.26E-09	8.48E-09	2.38E-07	8.2E-07	3.26E-07	6.53E-07	1.01E-08	1.41E-09	4.18E-09	3.26E-07
	U: 526.0000	U: 525.0000	U: 565.0000	U: 581.0000	U: 569.0000	U: 578.0000	U: 527.0000	U: 505.0000	U: 517.0000	U: 569.0000
	+	+	+	-	+	+	+	+	+	+
F11	2.15E-10	3.02E-11	1.61E-10	1.96E-10	2.87E-10	3.02E-11	1.09E-10	3.02E-11	8.15E-11	3.02E-11
	U: 485.0000	U: 465.0000	U: 482.0000	U: 484.0000	U: 488.0000	U: 465.0000	U: 478.0000	U: 465.0000	U: 475.0000	U: 465.0000
	+	+	+	+	+	+	+	+	+	+
F12	3.5E-09	3.02E-11	0.290472	0.520145	0.000399	3.02E-11	7.77E-09	3.02E-11	3.02E-11	9.92E-11
	U: 515.0000	U: 465.0000	U: 843.0000	U: 871.0000	U: 1155.0000	U: 465.0000	U: 524.0000	U: 465.0000	U: 465.0000	U: 477.0000
Total	+ :12, - :0, =:0	+ :12, - :0, =:0	+ :11, - :0, =:1	+ :10, - :1, =:1	+ :9, - :2, = :1 =:0	+ :12, - :0, =:0	+ :12, - :0, =:0	+ :12, - :0, =:0	+ :12, - :0, =:0	+ :12, - :0, =:0

**Table 15** Wilcoxon sum-rank test results

Function	SO	CPO	ROA	COA	GWO	WOA	MFO	ZOA	MTDE	SCA
F1	1.41E-11	4.2E-10	3.02E-11	3.02E-11	3.02E-11	3.02E-11	0.185761	3.02E-11	3.02E-11	3.02E-11
	U: 1365.0000	U: 492.0000	U: 465.0000	U: 465.0000	U: 465.0000	U: 465.0000	U: 825.0000	U: 465.0000	U: 465.0000	U: 465.0000
F2	-	+	+	+	+	+	=	+	+	+
	1.16E-07	0.589451	3.02E-11	0.520145	8.29E-06	1.39E-06	0.184328	0.008315	3.02E-11	3.02E-11
	U: 1274.0000	U: 952.0000	U: 465.0000	U: 959.0000	U: 613.0000	U: 588.0000	U: 825.0000	U: 736.0000	U: 465.0000	U: 465.0000
F3	-	=	+	=	+	+	=	+	+	+
	5.57E-10	3.02E-11	3.02E-11	5.19E-07	9.06E-08	3.02E-11	0.025081	3.02E-11	3.02E-11	3.02E-11
	U: 495.0000	U: 465.0000	U: 465.0000	U: 575.0000	U: 553.0000	U: 465.0000	U: 763.0000	U: 465.0000	U: 465.0000	U: 465.0000
F4	+	+	+	+	+	+	+	+	+	+
	0.002156	5.49E-11	9.92E-11	4.52E-10	0.1809	4.57E-09	4.69E-08	0.371077	3.02E-11	3.02E-11
	U: 707.0000	U: 471.0000	U: 477.0000	U: 493.0000	U: 824.0000	U: 518.0000	U: 545.0000	U: 854.0000	U: 465.0000	U: 465.0000
F5	+	+	+	+	=	+	+	=	+	+
	5.96E-05	3.02E-11	3.02E-11	5.57E-10	3.02E-11	3.02E-11	0.000398	3.02E-11	3.01E-11	3.02E-11
	U: 1185.0000	U: 465.0000	U: 465.0000	U: 495.0000	U: 465.0000	U: 465.0000	U: 675.0000	U: 465.0000	U: 465.0000	U: 465.0000
F6	+	+	+	+	+	+	+	+	+	+
	0.005828	9.26E-09	3.02E-11	3.69E-11	1.21E-10	4.5E-11	1.61E-10	6.52E-09	3.01E-11	3.02E-11
	U: 728.0000	U: 526.0000	U: 465.0000	U: 467.0000	U: 479.0000	U: 469.0000	U: 482.0000	U: 522.0000	U: 465.0000	U: 465.0000
F7	+	+	+	+	+	+	+	+	+	+
	6.53E-08	3.02E-11	3.02E-11	0.000812	1.85E-08	3.02E-11	1.29E-09	3.02E-11	3.01E-11	3.02E-11
	U: 549.0000	U: 465.0000	U: 465.0000	U: 688.0000	U: 534.0000	U: 465.0000	U: 504.0000	U: 465.0000	U: 465.0000	U: 465.0000
F8	+	+	+	+	+	+	+	+	+	+
	8.2E-07	5.49E-11	3.02E-11	1.61E-10	2.15E-10	3.69E-11	2.87E-10	6.07E-11	3.02E-11	3.69E-11

Table 15 (continued)

Function	SO	CPO	ROA	COA	GWO	WOA	MFO	ZOA	MTDE	SCA
	U: 581.0000	U: 471.0000	U: 465.0000	U: 482.0000	U: 485.0000	U: 467.0000	U: 488.0000	U: 472.0000	U: 465.0000	U: 467.0000
	+	+	+	+	+	+	+	+	+	+
F9	2.89E-11	3.02E-11	3.02E-11	6.72E-10	3.02E-11	3.02E-11	0.179042	3.02E-11	3.02E-11	3.02E-11
	U: 1365.0000	U: 465.0000	U: 465.0000	U: 1333.0000	U: 465.0000	U: 465.0000	U: 1005.0000	U: 465.0000	U: 465.0000	U: 465.0000
	-	+	+	+	+	+	=	+	+	+
F10	6.74E-06	2.92E-09	1.41E-09	2.6E-08	7.6E-07	2.39E-08	4.44E-07	1.11E-06	6.04E-07	8.2E-07
	U: 610.0000	U: 513.0000	U: 505.0000	U: 538.0000	U: 580.0000	U: 537.0000	U: 573.0000	U: 585.0000	U: 577.0000	U: 581.0000
	+	+	+	+	+	+	+	+	+	-
F11	0.373257	0.673495	3.02E-11	0.082357	3.16E-10	7.39E-11	0.205442	1.61E-10	3.02E-11	3.69E-11
	U: 975.0000	U: 886.0000	U: 465.0000	U: 797.0000	U: 489.0000	U: 474.0000	U: 829.0000	U: 482.0000	U: 465.0000	U: 467.0000
	=	=	+	=	+	+	=	+	+	+
F12	0.403538	3.02E-11	3.02E-11	0.000253	0.10547	1.17E-09	0.043505	3.02E-11	3.02E-11	3.02E-11
	U: 972.0000	U: 465.0000	U: 465.0000	U: 667.0000	U: 805.0000	U: 503.0000	U: 1052.0000	U: 465.0000	U: 465.0000	U: 465.0000
Total	+7, -3, =2	+10, -0, =:2	+12, -0, =:0	+10, -0, =:2	+10, -0, =:2	+12, -0, =:0	+7, -1, =:4	+11, -0, =:1	+12, -0, =:0	+11, -1, =:0

**Table 16** Wilcoxon sum-rank test results

Function	DOA	HHO	SCSO	GA	SA	AVOA	WSO	BBO	RIME	FOX	OHO
F1	3.02E-11 U: 465.0000	3.02E-11 U: 465.0000	3.02E-11 U: 465.0000	3.02E-11 U: 465.0000	3.02E-11 U: 465.0000	3.02E-11 U: 1365.0000	3.02E-11 U: 1365.0000	0.085 U: 798.0000	4.5E-11 U: 469.0000	3.02E-11 U: 1365.0000	3.02E-11 U: 465.0000
F2	+ 7.69E-08 U: 551.0000	+ 0.233989 U: 834.0000	+ 0.006097 U: 729.0000	+ 3.02E-11 U: 465.0000	+ 9.76E-10 U: 501.0000	- 0.067785 U: 1039.0000	- 2.67E-09 U: 1318.0000	= 0.001302 U: 1133.0000	+ 0.185767 U: 1005.0000	- 0.016955 U: 1077.0000	+ 3.02E-11 U: 465.0000
F3	+ 3.02E-11 U: 465.0000	= 3.02E-11 U: 465.0000	+ 3.02E-11 U: 465.0000	+ 3.02E-11 U: 465.0000	+ 3.02E-11 U: 465.0000	= 3.02E-11 U: 1155.0000	- 0.000399 U: 1155.0000	- 3.02E-11 U: 1365.0000	= 0.09049 U: 800.0000	+ 3.02E-11 U: 465.0000	+ 3.02E-11 U: 465.0000
F4	+ 2.78E-07 U: 567.0000	+ 1.75E-05 U: 624.0000	+ 1.6E-07 U: 560.0000	+ 3.02E-11 U: 465.0000	+ 2.61E-10 U: 487.0000	+ 1.31E-08 U: 530.0000	+ 0.002499 U: 1120.0000	- 0.074827 U: 794.0000	= 0.000399 U: 675.0000	+ 1.96E-10 U: 484.0000	+ 3.02E-11 U: 465.0000
F5	+ 3.02E-11 U: 465.0000	+ 3.02E-11 U: 465.0000	+ 3.02E-11 U: 465.0000	+ 3.02E-11 U: 465.0000	+ 3.02E-11 U: 465.0000	- 0.184751 U: 1005.0000	= 0.006972 U: 732.0000	= 9.26E-09 U: 526.0000	+ 3.02E-11 U: 465.0000	+ 3.02E-11 U: 465.0000	+ 3.02E-11 U: 465.0000
F6	+ 0.355472 U: 978.0000	+ 3.34E-11 U: 466.0000	+ 6.72E-10 U: 497.0000	+ 3.02E-11 U: 465.0000	+ 3.02E-11 U: 465.0000	+ 4.18E-09 U: 517.0000	= 3.02E-11 U: 1365.0000	+ 0.011228 U: 743.0000	+ 2.6E-08 U: 538.0000	+ 1.43E-08 U: 531.0000	+ 3.02E-11 U: 465.0000
F7	= 4.08E-11 U: 468.0000	+ 3.02E-11 U: 465.0000	+ 1.33E-10 U: 480.0000	+ 3.02E-11 U: 465.0000	+ 5.57E-10 U: 495.0000	+ 5.49E-11 U: 471.0000	- 0.00073 U: 686.0000	+ 3.16E-05 U: 633.0000	+ 0.039167 U: 775.0000	+ 3.02E-11 U: 465.0000	+ 3.02E-11 U: 465.0000

Table 16 (continued)

Function	DOA	HHO	SCSO	GA	SA	AVOA	WSO	BBO	RIME	FOX	OHO
F8	+	+	+	+	+	+	+	+	+	+	+
	4.08E-11 U: 468.0000	3.34E-11 U: 466.0000	3.69E-11 U: 467.0000	3.02E-11 U: 465.0000	6.72E-10 U: 497.0000	2.37E-10 U: 486.0000	1.17E-09 U: 503.0000	1.43E-05 U: 621.0000	0.000225 U: 665.0000	3.02E-11 U: 465.0000	3.02E-11 U: 465.0000
F9	+	+	+	+	+	+	+	+	+	+	+
	1.06E-07 U: 555.0000	3.02E-11 U: 465.0000	3.02E-11 U: 465.0000	3.02E-11 U: 465.0000	5.57E-10 U: 495.0000	5.15E-10 U: 1335.0000	1.2E-08 U: 1301.0000	3.02E-11 U: 1365.0000	0.051877 U: 1047.0000	5.46E-09 U: 520.0000	3.02E-11 U: 465.0000
F10	+	+	+	+	-	+	-	-	=	+	+
	1.43E-08 U: 531.0000	2.39E-08 U: 537.0000	2.19E-08 U: 536.0000	2.39E-08 U: 537.0000	0.000856 U: 689.0000	1.7E-08 U: 533.0000	0.002157 U: 707.0000	3.01E-07 U: 568.0000	2.77E-05 U: 631.0000	1.2E-08 U: 529.0000	9.92E-11 U: 477.0000
F11	+	+	+	+	-	+	+	+	+	+	+
	5.49E-11 U: 471.0000	8.99E-11 U: 476.0000	4.57E-09 U: 518.0000	3.02E-11 U: 465.0000	5.49E-11 U: 471.0000	0.695215 U: 888.0000	0.000377 U: 1156.0000	0.000356 U: 1157.0000	0.340288 U: 850.0000	1.02E-05 U: 616.0000	3.02E-11 U: 465.0000
F12	+	+	+	+	+	=	+	+	=	+	+
	3.02E-11 U: 465.0000	4.5E-11 U: 469.0000	2.13E-05 U: 627.0000	3.02E-11 U: 465.0000	2.92E-09 U: 513.0000	8.2E-07 U: 581.0000	5E-09 U: 519.0000	3.02E-11 U: 465.0000	0.000132 U: 656.0000	3.02E-11 U: 465.0000	3.02E-11 U: 465.0000
Total	+11, -0, =:1	+11, -0, =:1	+12, -0, =:0	+12, -0, =:0	+10, -2, =:0	+9, -1, =:2	+6, -5, =:1	+7, -3, =:2	+8, -0, =:4	+11, -1, =:0	+12, -0, =:0

**The use of AI** The authors declare that ChatGPT was used to improve the language, grammar, and clarity of the manuscript. The authors take full responsibility for the content of this work. The discussed methodology and results are all presented in the paper. Moreover, the proposed approach open source code implementation is available under <https://www.mathworks.com/matlabcentral/fileexchange/168366-shiod-eg-a-hybrid-success-history-intelligent-optimization>

**Competing interests** The authors declare no competing interests.

**Open Access** This article is licensed under a Creative Commons Attribution 4.0 International License, which permits use, sharing, adaptation, distribution and reproduction in any medium or format, as long as you give appropriate credit to the original author(s) and the source, provide a link to the Creative Commons licence, and indicate if changes were made. The images or other third party material in this article are included in the article's Creative Commons licence, unless indicated otherwise in a credit line to the material. If material is not included in the article's Creative Commons licence and your intended use is not permitted by statutory regulation or exceeds the permitted use, you will need to obtain permission directly from the copyright holder. To view a copy of this licence, visit <http://creativecommons.org/licenses/by/4.0/>.

## References

1. Engelbrecht AP (2006) Fundamentals of computational swarm intelligence. Wiley, New York
2. Fakhouri HN, Hudaib A, Sleit A (2020) Hybrid particle swarm optimization with sine cosine algorithm and Nelder-Mead simplex for solving engineering design problems. Arab J Sci Eng 45:3091–3109
3. Kennedy J, Eberhart R (1942) Particle swarm optimization. In: Proceedings of IEEE International Conference on Neural Networks. Perth, Australia 1948, 1995
4. Deb K, Pratap A, Agarwal S, Meyarivan T (2002) A fast and elitist multiobjective genetic algorithm: NSGA-II. IEEE Trans Evol Comput 6(2):182–197
5. Fakhouri HN, Awaysheh FM, Alawadi S, Alkhalailah M, Hamad F (2024) Four vector intelligent metaheuristic for data optimization. Computing 106(7):1–39
6. Karaboga D, Basturk B (2007) A powerful and efficient algorithm for numerical function optimization: artificial bee colony (ABC) algorithm. J Global Optim 39:459–471
7. Clerc M, Kennedy J (2002) The particle swarm-explosion, stability, and convergence in a multidimensional complex space. IEEE Trans Evol Comput 6(1):58–73
8. Wei J, Gu Y, Law KLE et al (2024) Adaptive position updating particle swarm optimization for UAV path planning. In: WiOpt
9. Lu B, Xie Z, Wei J et al (2025) MRBMO: an enhanced red-billed blue magpie optimization algorithm. Symmetry 17(8):1295. <https://doi.org/10.3390/sym17081295>
10. Wei J, Gu Y, Xie Z, Yan Y, Lu B, Li Z, Cheong N (2025) LSWOA: an enhanced whale optimization algorithm with Lévy flight and spiral flight for numerical and engineering design optimization problems. PLoS ONE 20(9):0322058. <https://doi.org/10.1371/journal.pone.0322058>
11. Wolpert DH, Macready WG (1997) No free lunch theorems for optimization. IEEE Trans Evol Comput 1(1):67–82
12. Fakhouri HN, Alawadi S, Awaysheh FM, Hamad F (2023) Novel hybrid success history intelligent optimizer with gaussian transformation: application in CNN hyperparameter tuning. Clust Comput 27:3717–3739
13. Yang X-S (2020) Nature-Inspired Optimization Algorithms. Academic Press, London
14. Reynolds RG (1994) An introduction to cultural algorithms. In: Proceedings of the Third Annual Conference on Evolutionary Programming, World Scientific, vol 24, pp 131–139
15. Ahmadi S-A (2017) Human behavior-based optimization: a novel metaheuristic approach to solve complex optimization problems. Neural Comput Appl 28:233–244
16. Askari Q, Younas I, Saeed M (2020) Political optimizer: a novel socio-inspired meta-heuristic for global optimization. Knowl Based Syst 195:105709
17. Rao RV, Savsani VJ, Vakharia DP (2011) Teaching-learning-based optimization: a novel method for constrained mechanical design optimization problems. Comput Aided Design 43:303–315

18. Trojovská E, Dehghani M (2022) A new human-based metaheuristic optimization method based on mimicking cooking training. *Sci Rep* 12:14861
19. Wang X, Xu J, Huang C (2023) Fans optimizer: a human-inspired optimizer for mechanical design problems optimization. *Expert Syst Appl* 228:120242
20. Matoušová I, Trojovský P, Dehghani M, Trojovská E, Kostra J (2023) Mother optimization algorithm: a new human-based metaheuristic approach for solving engineering optimization. *Sci Rep* 13:10312
21. Abualigah L, Diabat A, Mirjalili S, Abd Elaziz M, Gandomi AH (2021) The arithmetic optimization algorithm. *Comput Methods Appl Mech Eng* 376:113609
22. Talatahari S, Azizi M (2021) Chaos game optimization: a novel metaheuristic algorithm. *Artif Intell Rev* 54:917–1004
23. Zhao W, Wang L, Zhang Z (2019) Supply-demand-based optimization: a novel economics-inspired algorithm for global optimization. *IEEE Access* 7:73182–73206
24. Kang F, Li J, Ma Z (2011) Rosenbrock artificial bee colony algorithm for accurate global optimization of numerical functions. *Inf Sci* 181:3508–3531
25. Dorigo M, Birattari M, Stutzle T (2006) Ant colony optimization. *IEEE Comput Intell Mag* 1:28–39
26. Kennedy J, Eberhart R (1995) Particle swarm optimization. In: *Proceedings of ICNN'95—International Conference on Neural Networks*, 4, pp 1942–1948
27. Mirjalili S, Mirjalili SM, Lewis A (2014) Grey wolf optimizer. *Adv Eng Softw* 69:46–61
28. Wei J, Gu Y, Lu B, Cheong N (2025) RWOA: a novel enhanced whale optimization algorithm for numerical optimization and engineering design problems. *PLoS ONE* 20(4):0320913. <https://doi.org/10.1371/journal.pone.0320913>
29. Gu Y, Wei J, Li Z, Lu B, Pan S, Cheong N (2025) GWOA: a multi-strategy enhanced whale optimization algorithm for engineering design optimization. *PLoS ONE* 20(9):0322494. <https://doi.org/10.1371/journal.pone.0322494>
30. Wei J, Gu Y, Yan Y, Li Z, Lu B, Pan S, Cheong N (2025) LSEWOA: an enhanced WOA with multi-strategy for numerical and engineering optimization. *Sensors* 25(7):2054. <https://doi.org/10.3390/s25072054>
31. Qawaqneh H, Alomari KM, Alomari SA, Bektemyssova GU, Smerat A, Montazeri Z, Dehghani MJ, Malik OP, Eguchi K (2025) Kakapo optimization algorithm (KOA): a novel bio-inspired metaheuristic for optimization applications. *Int J Intell Eng Syst* 18(11):913–929. <https://doi.org/10.22266/ijies2025.1231.56>
32. Qawaqneh H, Alomari KM, Alomari SA, Bektemyssova GU, Smerat A, Montazeri Z, Dehghani MJ, Malik OP, Eguchi K (2025) Black-breasted lapwing algorithm (BBLA): a novel nature-inspired metaheuristic for solving constrained engineering optimization. *Int J Intell Eng Syst* 18(11):581–597. <https://doi.org/10.22266/ijies2025.1231.36>
33. Wang X, Yao L (2025) Cape lynx optimizer: a novel metaheuristic algorithm for enhancing wireless sensor network coverage. *Measurement* 256:118361. <https://doi.org/10.1016/j.measurement.2025.118361>
34. Chen S, Yang G, Cui G, Dong X (2025) Raindrop optimizer: a novel nature-inspired metaheuristic algorithm for artificial intelligence and engineering optimization 15(1) <https://doi.org/10.1038/s41598-025-15832-w>. All Open Access; Gold Open Access; Green Accepted Open Access; Green Open Access
35. Lang Y, Gao Y, Chen T, Wang H (2026) Centered collision optimizer: a novel and efficient physics-based metaheuristic optimization algorithm for solving complex real-world engineering optimization problems. *Comput Methods Appl Mech Eng* 448:118491. <https://doi.org/10.1016/j.cma.2025.118491>
36. Fakhouri HN, Hudaib AA, Fakhouri SN, Hamad FF, Alkhalailah MS (2025) Aurora intelligent metaheuristic: a novel space-inspired optimizer. *SN Comput Sci* 6:8. <https://doi.org/10.1007/s42979-025-04512-1>
37. Rodan A, Sanjalawe YK, Tino P (2025) Three-body deterministic optimizer (TBD): a novel non-random, nature-inspired metaheuristic for engineering design and hyperparameter optimization. *Evolut Intell*. <https://doi.org/10.1007/s12065-025-01107-w>
38. Wang J, Shang Z (2026) Traffic jam optimizer: a novel swarm-based metaheuristic algorithm for solving global optimization problems. *Appl Math Modell* 150:116410. <https://doi.org/10.1016/j.apm.2025.116410>
39. Xia Y, Ji Y (2025) Application of a novel metaheuristic algorithm inspired by Adam gradient descent in distributed permutation flow shop scheduling problem and continuous engineering

- problems 15(1) <https://doi.org/10.1038/s41598-025-01678-9>. All Open Access; Gold Open Access; Green Accepted Open Access; Green Open Access
40. Khaire UM, Hiremath SR, Londhe K, Manjusha CB, Mahapatra AS (2026) Hybrid butter-flower algorithm: Novel metaheuristic optimization algorithm, vol 477. <https://doi.org/10.1016/j.cam.2025.117148>
  41. Micev M, Calasan MP, Tokic A (2026) Novel approach for estimation of light-emitting diode lamp parameters based on hybrid metaheuristic algorithms. *J Comput Electron* 25:14
  42. Ding S, Lin J, Zhou W, Zhang J, Chen H (2025) A novel assembly sequence evaluation and planning method in high-speed winding spindle assembly using hybrid metaheuristic algorithm. *Proc Inst Mech Eng Part B J Eng Manuf* 239(14):2057–2071. <https://doi.org/10.1177/09544054241308664>
  43. Tian D (2025) A novel quality of service-aware service composition method for cloud computing using enhanced prairie dog metaheuristic optimization algorithm. *J Eng Appl Sci*. <https://doi.org/10.1186/s44147-025-00717-6>
  44. Mohamed MI, Yousef AM, Hafez AA (2025) A novel metaheuristic optimizer GPSED via artificial intelligence for reliable economic dispatch 15(1) <https://doi.org/10.1038/s41598-025-06648-9>. All Open Access; Gold Open Access; Green Accepted Open Access; Green Open Access
  45. Su R, Lin M, Chen G, Chen Y, Hu N, Wang J, Ye Z (2026) Mixture optimization of mechanical, economical, and environmental objectives for a novel industrial waste-based geopolymer: Combining ensemble learning with metaheuristic algorithms. *J Mater Civ Eng*. <https://doi.org/10.1061/JMCEE7.MTENG-20626>
  46. Zhou J, Xu M, Li C (2025) Prediction of dam failure peak outflow using a novel explainable random forest based on metaheuristic algorithms. *J Hydrol* 662:133767. <https://doi.org/10.1016/j.jhydrol.2025.133767>
  47. Xu S, Tang Y (2025) Short-term wind power forecasting: a novel enhanced gate-based deep-learning model containing a metaheuristic algorithm with an intelligent position navigation optimization strategy. *J Energy Eng*. <https://doi.org/10.1061/JLEED9.EYENG-6163>
  48. Badana M, Beesetti KK, Sundari MR, Ramya P, Rao GS (2025). A novel hybrid deep learning framework with metaheuristic optimization for accurate software effort estimation. <https://doi.org/10.1007/s42979-025-04459-3>
  49. Guler NU, Bakir H, Yumurtaci Z, Ağbulut Ü (2025) Syngas production through forest waste gasification and prediction of its species using advanced novel metaheuristic driven hybrid machine learning algorithms. *Int J Hydrogen Energy* 196:152529
  50. Sabry M, Elbaz M, Alzabni WO (2025) Novel metaheuristic optimized latent diffusion framework for automated oral disease detection in public health screening. *Sci Rep*. <https://doi.org/10.1038/s41598-025-25739-1>
  51. Wei J, Gu Y, Law KLE, Cheong N (2024) Adaptive position updating particle swarm optimization for UAV path planning. In: *Proceedings of the 22nd IEEE International Symposium on Modeling and Optimization in Mobile, Ad Hoc, and Wireless Networks (WiOpt)*, pp 124–131
  52. Talbi E-G (2009) *Metaheuristics: from design to implementation*. Wiley, New York
  53. Blum C, Puchinger J, Raidl GR, Roli A (2011) Hybrid metaheuristics in combinatorial optimization: a survey. *Appl Soft Comput* 11(6):4135–4151
  54. Fakhouri HN, Hamad F, Alawamrah A (2021) Success history intelligent optimizer. *J Supercomput* 78(5):6461–6502. <https://doi.org/10.1007/s11227-021-04093-9>
  55. Falahah IA, Al-Baik O, Alomari S, Bektemyssova G, Gochhait S et al (2024) Frilled lizard optimization: A novel bio-inspired optimizer for solving engineering applications. *Comput Mater Contin* 79(3):3631–3678. <https://doi.org/10.32604/cmc.2024.053189>
  56. Dhiman G, Kaur A (2019) STOA: a bio-inspired based optimization algorithm for industrial engineering problems. *Eng Appl Artif Intell* 82:148–174. <https://doi.org/10.1016/j.engappai.2019.04.024>
  57. Dhiman G, Kumar V (2019) Seagull optimization algorithm: theory and its applications for large-scale industrial engineering problems. *Knowl-Based Syst* 165:169–196. <https://doi.org/10.1016/j.knsys.2018.12.032>
  58. Fakhouri HN, Awaysheh FM, Alawadi S, Alkhalaileh M, Hamad F (2024) Four vector intelligent metaheuristic for data optimization. *Computing* 106:2321–2359. <https://doi.org/10.1007/s00607-024-01287-w>

59. Das B, Mukherjee V, Das D (2020) Student psychology based optimization algorithm: a new population based optimization algorithm for solving optimization problems. *Adv Eng Softw* 146:102804. <https://doi.org/10.1016/j.advengsoft.2020.102804>
60. Abualigah L, Yousri D, Elaziz MA, Ewees AA, Al-qaness MA, Gandomi AH (2021) Aquila optimizer: a novel meta-heuristic optimization algorithm. *Comput Ind Eng* 157:107250. <https://doi.org/10.1016/j.cie.2021.107250>
61. Kaveh A, Zaerreza A (2020) Shuffled shepherd optimization method simplified for reducing the parameter dependency. *Iran J Sci Technol Trans Civil Eng* 44:1205–1218. <https://doi.org/10.1007/s40996-020-00428-3>
62. Abdulrab H, Hussin FA, Ismail I, Assad M, Awang A, Shutari H, Arun D (2024) Energy efficient optimal deployment of industrial wireless mesh networks using transient trigonometric Harris hawks optimizer. *Heliyon* 10(7):08513. <https://doi.org/10.1016/j.heliyon.2023.e08513>
63. Khishe M, Mosavi MR (2020) Chimp optimization algorithm: a new metaheuristic optimizer for solving optimization problems. *Expert Syst Appl* 149:113338. <https://doi.org/10.1016/j.eswa.2020.113338>
64. Hashim FA, Hussien AG et al (2022) Snake optimizer: a novel meta-heuristic optimization algorithm. *Knowl Based Syst* 242:108320. <https://doi.org/10.1016/j.knsys.2022.108320>
65. Abdel-Basset M al\* (2024) Crested porcupine optimizer: a new nature-inspired metaheuristic algorithm. Article in press (Introduced in 2024 by Abdel-Basset et al.)
66. Jia H, Peng X, Lang C (2021) Remora optimization algorithm. *Expert Syst Appl* 185:115665. <https://doi.org/10.1016/j.eswa.2021.115665>
67. Pierezan J, S Coelho L (2018) Coyote optimization algorithm: a new metaheuristic for global optimization problems. In: *Proceedings of IEEE Congress on Evolutionary Computation (CEC)*, pp 2633–2640. <https://doi.org/10.1109/CEC.2018.8477769>
68. Mirjalili S, Mirjalili SM, Lewis A (2014) Grey wolf optimizer. *Adv Eng Softw* 69:46–61. <https://doi.org/10.1016/j.advengsoft.2013.12.007>
69. Mirjalili S, Lewis A (2016) The Whale Optimization Algorithm. *Adv Eng Softw* 95:51–67. <https://doi.org/10.1016/j.advengsoft.2016.01.008>
70. Mirjalili S (2015) Moth-flame optimization algorithm: a novel nature-inspired heuristic paradigm. *Knowl-Based Syst* 89:228–249. <https://doi.org/10.1016/j.knsys.2015.07.006>
71. Trojovská E, Dehghani M, Trojovský P (2022) Zebra optimization algorithm: a new bio-inspired optimization algorithm for solving optimization problems. *IEEE Access* 10:49445–49473. <https://doi.org/10.1109/ACCESS.2022.3172278>
72. Nadimi-Shahraki MH, Taghian S, Mirjalili S, Faris H (2020) MTDE: an effective multi-trial vector-based differential evolution algorithm and its applications for engineering design problems. *Appl Soft Comput* 97:106761. <https://doi.org/10.1016/j.asoc.2020.106761>
73. Mirjalili S (2016) SCA: a sine cosine algorithm for solving optimization problems. *Knowl-Based Syst* 96:120–133. <https://doi.org/10.1016/j.knsys.2015.12.022>
74. Zhao S, Zhang T, Wang X, Chen Z (2022) Dandelion optimizer: a nature-inspired metaheuristic algorithm for engineering applications. *Eng Appl Artif Intell* 114:105075. <https://doi.org/10.1016/j.engappai.2022.105075>
75. Heidari AA, Mirjalili S, Faris H, Aljarah I, Mafarja M, Chen H (2019) Harris hawks optimization: algorithm and applications. *Futur Gener Comput Syst* 97:849–872. <https://doi.org/10.1016/j.future.2019.02.028>
76. Seyedabbasi A, Kiani F (2023) Sand cat swarm optimization: a nature-inspired algorithm to solve global optimization problems. *Eng Comput* 39(4):3755–3777. <https://doi.org/10.1007/s00366-022-01685-7>
77. Holland JH (1975) *Adaptation in natural and artificial systems*. University of Michigan Press, Ann Arbor
78. Kirkpatrick S, Gelatt CD, Vecchi MP (1983) Optimization by simulated annealing. *Science* 220(4598):671–680. <https://doi.org/10.1126/science.220.4598.671>
79. Abdollahzadeh B, Gharehchopogh FS, Mirjalili S (2021) African vultures optimization algorithm: a new nature-inspired metaheuristic algorithm for global optimization problems. *Comput Ind Eng* 158:107408. <https://doi.org/10.1016/j.cie.2021.107408>
80. Simon D (2008) Biogeography-based optimization. *IEEE Trans Evol Comput* 12(6):702–713. <https://doi.org/10.1109/TEVC.2008.919004>
81. Su W, Chen H al\* (2023) RIME: a physics-based optimization algorithm inspired by rime ice growth (2023). Presented as a novel algorithm in (Su et al.)

82. Mohammed H, Rashid T (2023) Fox: a fox-inspired optimization algorithm. *Appl Intell* 53:1030–1050. <https://doi.org/10.1007/s10489-022-03533-0>
83. Zhang J (2025) Oriolus-inspired heuristic optimization algorithm based on foraging behavior. Preprint (ResearchGate). <https://doi.org/10.13140/RG.2.2.12504.35844>
84. Derrac J, García S, Molina D, Herrera F (2011) A practical tutorial on the use of nonparametric statistical tests as a methodology for comparing evolutionary and swarm intelligence algorithms. *Swarm Evol Comput* 1(1):3–18. <https://doi.org/10.1016/j.swevo.2011.02.002>
85. Demšar J (2006) Statistical comparisons of classifiers over multiple data sets. *J Mach Learn Res* 7:1–30
86. Carrasco J, García S, Rueda M, Herrera F (2020) Recent trends in the use of statistical tests for comparing metaheuristics. *Swarm Evolut Comput*. Preprint available at [arXiv:2002.09227](https://arxiv.org/abs/2002.09227)

**Publisher's Note** Springer Nature remains neutral with regard to jurisdictional claims in published maps and institutional affiliations.

## Authors and Affiliations

**Sadi Alawadi<sup>1</sup> · Hussam N. Fakhouri<sup>2</sup> · Fahed Alkhabbas<sup>3</sup> · Victor R. Kebande<sup>1</sup> · Feras M. Awaysheh<sup>4</sup> · Abbas Cheddad<sup>4</sup>**

✉ Sadi Alawadi  
sadi.alawadi@bth.se

Hussam N. Fakhouri  
hussam.fakhouri@uop.edu.jo

Fahed Alkhabbas  
fahed.alkhabbas@mau.se

Victor R. Kebande  
victor.kebande@bth.se

Feras M. Awaysheh  
feras.awaysheh@ut.ee

Abbas Cheddad  
abbas.cheddad@ut.ee

<sup>1</sup> School of Computer Science, Blekinge Tekniska Högskola, 37179 Karlskrona, Blekinge, Sweden

<sup>2</sup> Data Science and Artificial Intelligence Department, Faculty of Information Technology, University of Petra, Amman, Jordan

<sup>3</sup> Sustainable Digitalisation Research Centre, Malmö University, Malmö, Sweden

<sup>4</sup> Institute of Computer Science, Delta Research Centre, University of Tartu, Tartu, Estonia